4. Mean zonal and meridional circulations

The tropics belongs to the meridional variability, which is next to vertical but clearly more remarkable than zonal. Thus we define (Eulerian-) *zonal mean* and disturbance:

$$\overline{(\ \ )} \equiv \frac{1}{2\pi}\int_0^{2\pi}(\ \ )d\lambda = \frac{1}{2\pi a}\int_0^{2\pi a}(\ \ )dx\,, \qquad (\ \ )' \equiv (\ \ ) - \overline{(\ \ )}, \quad \frac{\partial\overline{(\ \ )}}{\partial x} = 0, \tag{4.1}$$

where λ is longitude and $a = 6.37\times10^6$ m is the Earth's radius. This definition is valid and useful for the atmosphere which has no horizontal boundaries like coastlines of the oceans. The zonal continuity is a necessary condition also for the atmospheric zonal uniformity and zonal flow dominance.

Applying (4.1) to (3.13) – (3.17) and neglecting minor terms, we obtain zonal-mean "*Quasi-geostrophic*" equations:

$$\frac{\partial\overline{u}}{\partial t} + \left(\frac{\partial\overline{u}}{\partial y} - f\right)\overline{v} + \frac{\partial\overline{u}}{\partial z}\overline{w} = \overline{G}, \tag{4.2}$$

$$f\overline{u} + \frac{\partial\overline{\phi}}{\partial y} = 0, \tag{4.3}$$

$$\frac{\partial\overline{\phi}}{\partial z} = \frac{R\overline{T}}{H}, \tag{4.4}$$

$$\frac{\partial\overline{v}}{\partial y} + \frac{1}{\rho_0}\frac{\partial\rho_0\overline{w}}{\partial x} = 0, \tag{4.5}$$

$$\frac{\partial\overline{T}}{\partial t} + \frac{\partial\overline{T}}{\partial y}\overline{v} + \left(\frac{\partial\overline{T}}{\partial z} + \Gamma\right)\overline{w} = \overline{Q}. \tag{4.6}$$

In this system the geostrophic component of $\overline{v}$ is omitted, because it must be balanced with $\partial\overline{\phi}/\partial x = 0$. The vertical acceleration is neglected by the hydrostatic approximation. Therefore, the zonal mean *meridional circulation* ($\overline{v}$, $\overline{w}$) does not appear in the meridional and vertical components (4,3), (4.4) of the equation of motion, and is driven by *ageostrophic* terms (friction to the zonal flow $\overline{u}$, etc.) in the zonal momentum equation (4.2) and by diabatic heating in the thermodynamic equation (4.3). Including them, the forcing terms $\overline{G}$ and $\overline{Q}$ consist of zonal mean of those in original equations ($\overline{F}$ and $(\overline{J} + L\overline{s})/C_p$) and nonlinear products of disturbance quantities (shown in Chapters 5 and 6).

In order to describe/solve dynamical issues easily, we may use so-called "β-plane approximation":

$$f(y) = \beta y\,, \qquad \beta \equiv \left.\frac{df}{dy}\right|_{y=0} = \frac{2\Omega}{a}, \tag{4.7}$$

where β is called the Rossby parameter or simply the "beta"-effect. Near the equator the Coriolis parameter f vanishes, but its gradient β becomes maximum. Considering this specialty (4.7) is particularly called the *equatorial β-plane approximation*. Under this approximation, the *absolute angular momentum* may be written as

$$M(y) = \Omega(a^2 - y^2) + au = a\left[\frac{\beta}{2}(a^2 - y^2) + u\right]. \tag{4.8}$$

Then the zonal equation of motion (4.2) may be rewritten as the zonal-mean angular momentum conservation law:

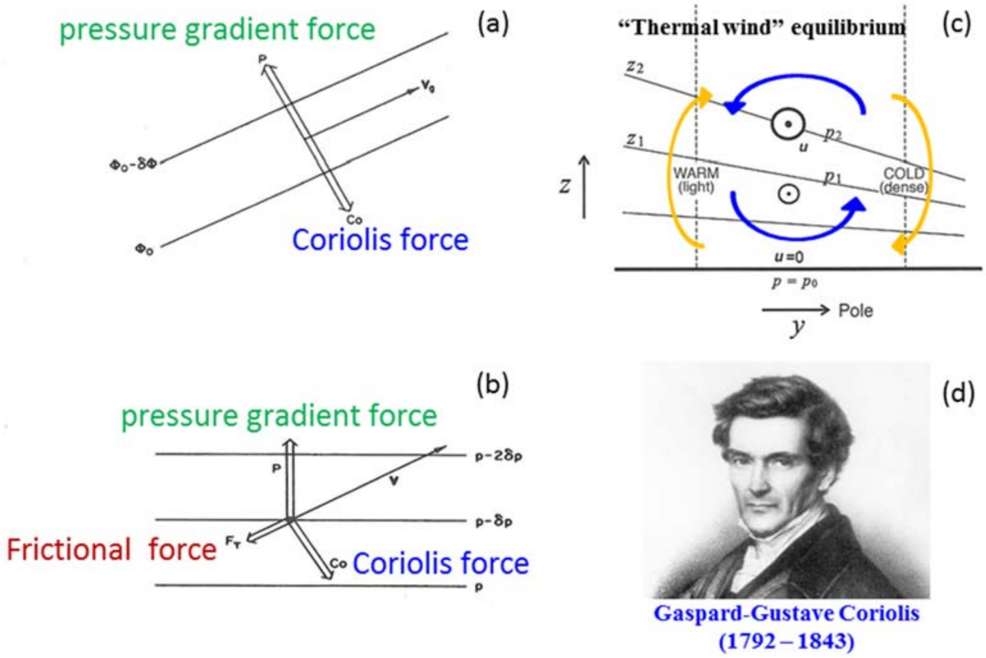

Fig. 4.1 (a) Geostrophic equilibrium, (b) surface wind including friction (these two modified from Holton, 1992), (c) thermal wind equilibrium as a balance between buoyancy (orange) and Coriolis (blue) torques (modified from Marshall and Plumb, 2008), all in the northern hemisphere, and (d) a portrait of Coriolis (originally from Académie des Sciences Paris).

$$\left(\frac{\partial}{\partial t}+\bar{v}\frac{\partial}{\partial y}+\bar{w}\frac{\partial}{\partial z}\right)\bar{M}=a\bar{G}, \tag{4.9}$$

or, combined with the continuity equation (4.5),

$$\frac{\partial \rho_0\bar{M}}{\partial t}=-\left(\frac{\partial \rho_0\bar{M}\bar{v}}{\partial y}+\frac{\partial \rho_0\bar{M}\bar{w}}{\partial z}\right)+a\rho_0\bar{G}. \tag{4.10}$$

These equations show, if no acceleration/friction ($\bar{G}=0$), that $\bar{M}$ is a Lagrangian invariant for any parcel moving in the mean meridional plane, and that $\rho_0\bar{M}$ is an Eularian conserved quantity at any point if there are no divergence of momentum flux ($\rho_0\bar{M}\bar{v}$, $\rho_0\bar{M}\bar{w}$).

4.1. Trade wind (Equatorial easterly)

The steady free solution ($\partial/\partial t=0$; $\bar{G}$, $\bar{Q}=0$) of (4.2) – (4.6) is trivial: $\bar{u}$, $\bar{T}$ and $\bar{\phi}$ satisfying the geostrophic and hydrostatic equilibria, (4.3) and (4.4), and no meridional circulation ($\bar{v}=\bar{w}=0$). Making $\partial(25)/\partial z-\ \partial(26)/\partial y$, we obtain the so-called *thermal wind equilibrium*:

$$f\frac{\partial\bar{u}}{\partial z}+\frac{R}{H}\frac{\partial\bar{T}}{\partial y}=0, \tag{4.11}$$

which represents a "torque balance" between the vertical difference of meridional centrifugal (Coriolis) force and the meridional difference of buoyancy (gravity) force[17]. Near the equator ($f\to 0$), we have $\partial\bar{T}/\partial y\to 0$, and applications of the L'Hospital theorem[18] to (4.3) and (4.11) provide

[17]For a superrotation ($u \gtrsim 2\Omega a$) multiple equilibria appear, because the centrifugal force becomes nonlinear (Matsuda, 1980).
[18]If $f(x)/g(x)\to 0/0$ at $x\to a$, then $f(a)/g(a)=f'(a)/g'(a)$.

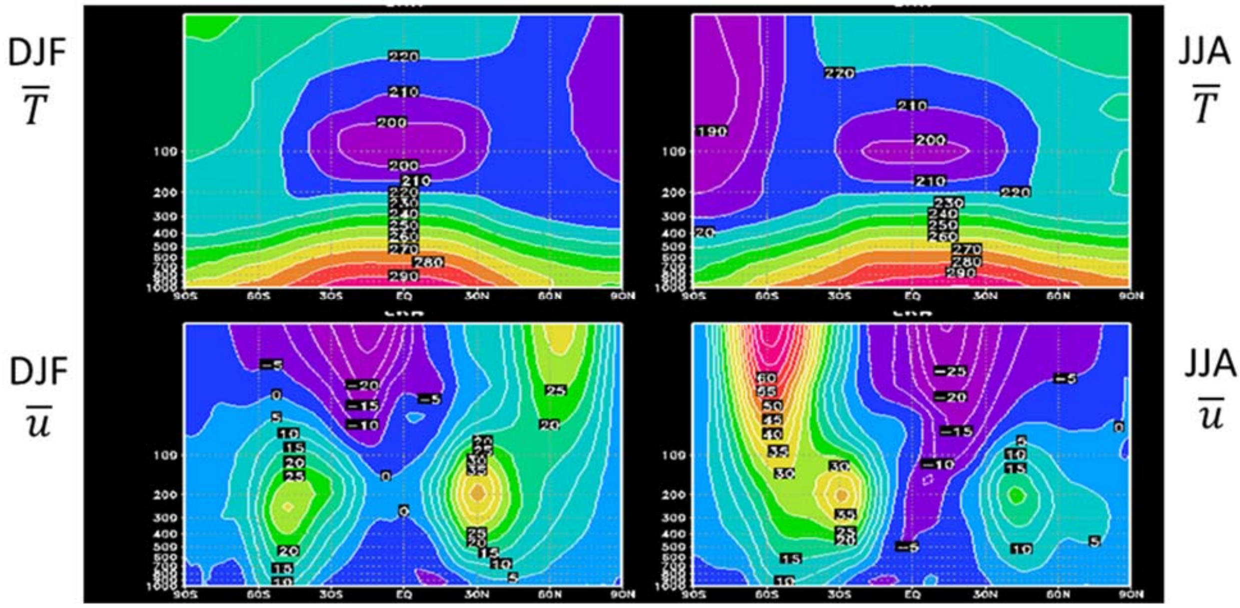

Fig. 4.2 Meridional-vertical (0 – 30 km) distributions of climatological zonal mean temperature (top) and zonal wind (bottom) for December-February (left) and June-August (right) (Kimoto, 2004, personal communication).

$$\beta\overline{u} + \frac{\partial^2\overline{\phi}}{\partial y^2} = 0\,, \qquad \beta\frac{\partial\overline{u}}{\partial z} + \frac{R}{H}\frac{\partial^2\overline{T}}{\partial y^2} = 0.$$

Actual meridional-vertical distributions of $\overline{u}$ are shown in lower panels of Fig. 4.2. In general easterly is dominant in the tropics, which corresponds to the zonal-mean zonal component of northeasterly/southeasterly *trade winds*[19] blowing from the northern/southern *subtropical anticyclones* to the *intertropical convergence zone* (ITCZ) in surface weather maps. This feature is similar to Hadley's classical consideration, except for the actual easterly dominance throughout the tropical troposphere[20] (cf. Section 4.3). A maximum of the trade wind is in the lower troposphere in the winter hemispheric side of the equator, which is opposite to the ITCZ shifted from the equator to the summer hemispheric side. Winter monsoon in the Indo-Pacific sector may contribute this distribution (Section 4.4). Another one is around the tropopause roughly above the ITCZ, which seems to be connected to the summer stratospheric easterly, although the equatorial lower stratospheric winds are not so simple due to a quasi-biennial-vertical variation (Sections 4.5 and 5.4).

If we consider a friction[21] to the zonal flow in (4.10):

$$\overline{G} \approx -\alpha'\overline{u} \tag{4.12}$$

becomes positive (westerly or rotation-wise acceleration) in the low latitude easterly ($\overline{u} < 0$) and negative (easterly or anti-rotation acceleration) in the mid latitude westerly ($\overline{u} > 0$), which suggests a cycle of the absolute angular momentum between the lower and mid latitudes. In the latitudes apart from the equator the zonal friction $\overline{G}$ must be balanced with the Coriolis term on the meridional flow (Section 4.3; also seen in Fig. 4.1(b)), which was not expected by Hadley.

[19]Since Columbus' pioneering cruise in 1492 European traders' sailing ships uses this prevailing wind for going to Americas.
[20]"Abnormally strong" westerlies appear with intraseasonal variations (Section 6.4), monsoons (4.4) and El Niño phases (5.3).
[21]This parametrization (formally similar to Newtonian cooling (3.6) on $\overline{T}$) is called the Rayleigh friction.

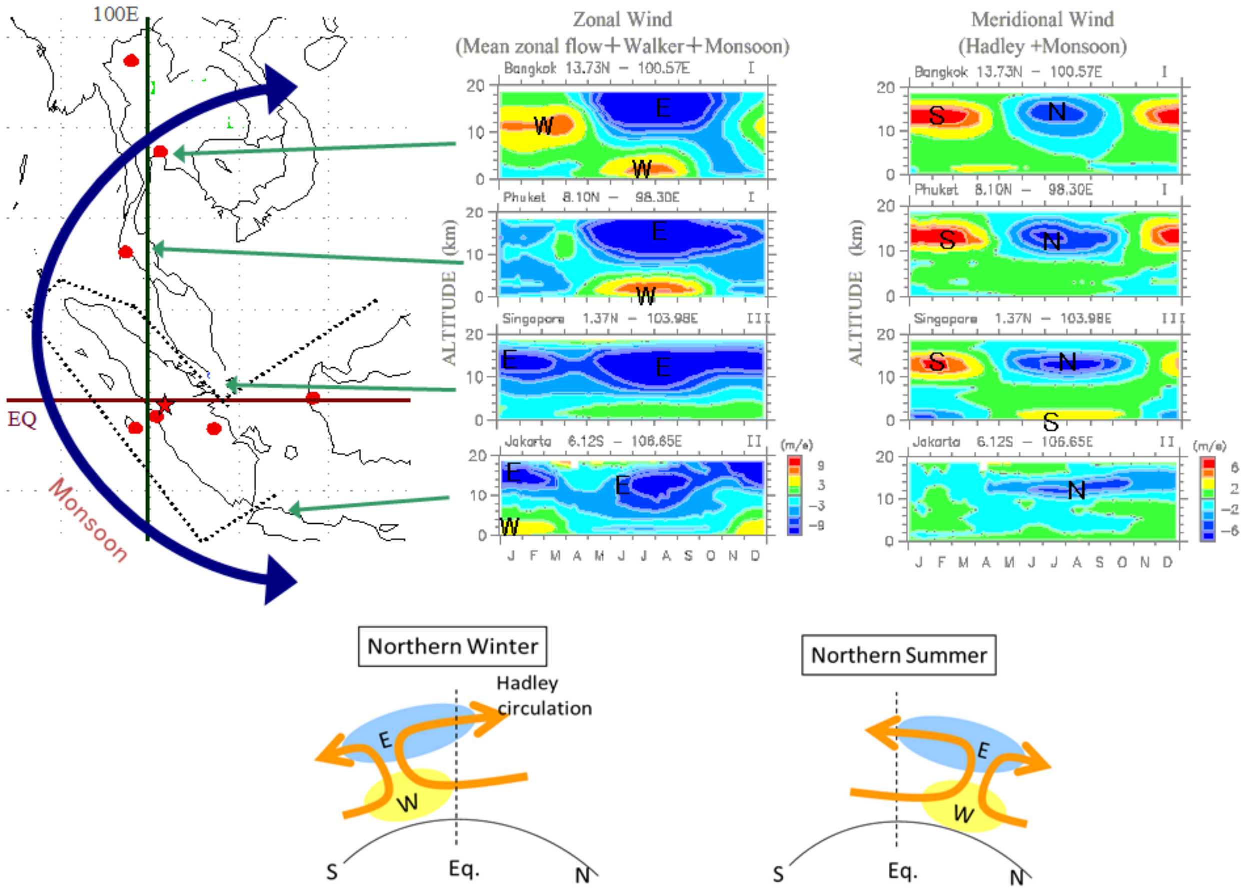

Fig. 4.3 Seasonal-vertical variations of zonal (upper middle) and meridional (upper right) winds at Bangkok, Phuket, Singapore and Jakarta (upper left), showing semiannual variations of zonal wind associated with an annual shift of Hadley circulation (lower panels) (modified from Okamoto et al., 2003).

Easterly corresponds to an anti-cyclonic circulation around a pole, and the pressure gradient and zonal disturbance stability must be weaker than cyclonic circulation or westerly[22]. Actually $\partial\overline{\phi}/\partial y$, $\partial\overline{T}/\partial y$, $\overline{u}$ and $\partial\overline{u}/\partial z$ are usually all smaller than mid-latitude, and baroclinic instability (generating extratropical cyclones in mid-latitudes) does not appear in the tropics. Thus $\overline{G}$ is smaller and conservation of $\overline{M}$ is better (except for the stratosphere and above, where $\overline{G}$ associated with waves propagating upward from the troposphere generate periodic variations of $\overline{M}$ or $\overline{u}$, as discussed in Section 5.4).

Actual equatorial easterly has zonal and temporal variabilities, associated with ENSO/IOD (interannual variations over the Pacific and Indian Oceans), monsoon (annual cycle), intraseasonal variations (ISVs). The annual intensification/shift of Hadley cells (Section 4.2) associated with monsoon (Section 4.3) may induce a semiannual intensification of equatorial easterly jet (Okamoto et al., 2003) (Fig.4.3).

[22] If we include centrifugal force discussed in Chapter 2, (4.3) is rewritten as the following so-called "gradient wind balance":

$$(2\Omega \sin\varphi)\cdot\overline{u} + \frac{\overline{u}^2}{a}\tan\varphi + \frac{\partial\overline{\phi}}{\partial y} = 0 \qquad \therefore\ \overline{u} = -a\Omega\cos\varphi \pm \sqrt{a^2\Omega^2\cos^2\varphi - \cot\varphi\frac{\partial\overline{\phi}}{\partial\varphi}}$$

which requests $\partial\overline{\phi}/\partial|\varphi| \le (1/2)a^2\Omega^2\sin 2|\varphi|$ and an anti-cyclonic pressure gradient $(\partial\overline{\phi}/\partial|\varphi| > 0)$ must have an upper limit.

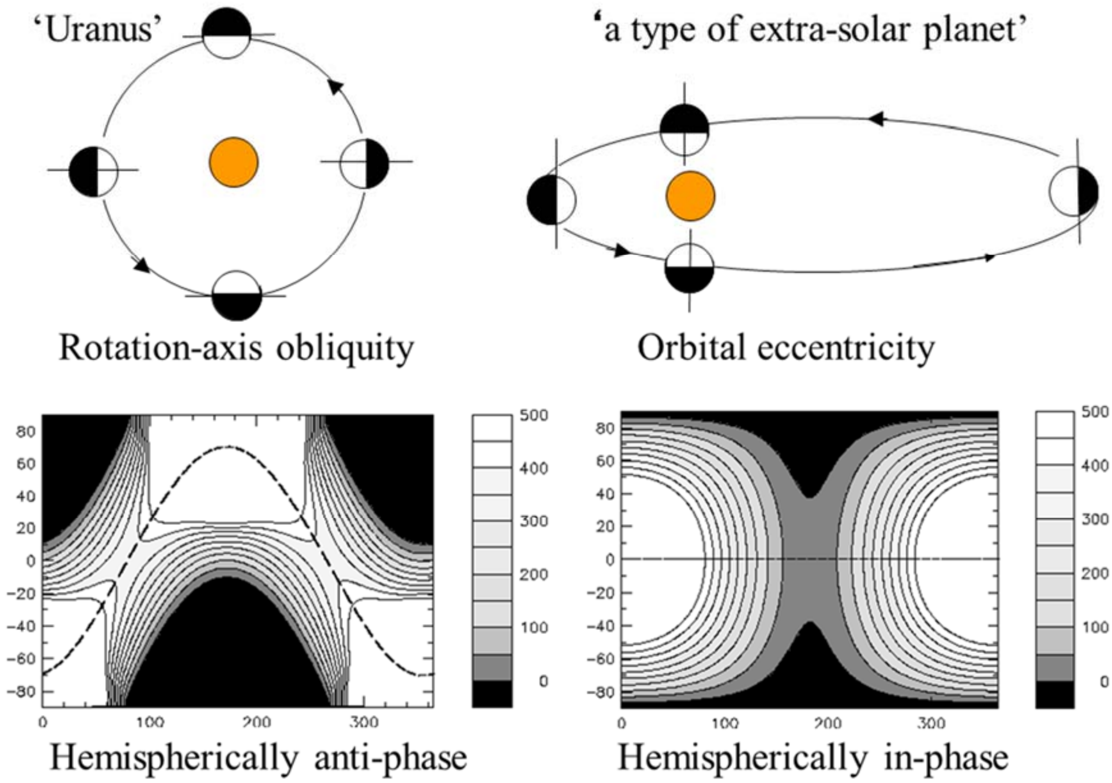

Fig. 4.4 Two extreme cases of planetary rotation/revolution (upper panels) causing seasonal-meridional variations of daily-mean insolation (lower panels). Insolation is calculated under the annual mean value given by the solar constant of actual Earth (as shown later in Fig. 4.5).

The meridional variability including tropical specialty is basically due to the Earth's sphericity and rotation, which govern the solar irradiance and the Coriolis force. As shown in Fig. 1.4(a) the solar irradiance contributes to the heating term J or $\overline{Q}$ through the parasol effect, surface heating and boundary-layer processes, which are complex (e.g., Hartmann, 1994; Stull, 1988). However, observations support that its variability is mainly dependent on its value calculated by the astronomical formula (I_s given in Section 6.1). For the solar heating, since the Earth's rotation relative to Sun is just 1 solar day = 24 h = 86,400 s, the zonal mean is the daily average:

$$\overline{Q}^{\text{day}} \dot{\propto} \overline{I_s}^{\text{day}} = \frac{1}{1\ \text{solar day}} \int_{-h_0}^{h_0} I_s\, dt = \frac{I_{s0}}{\pi} \left(\frac{\overline{d}}{d}\right)^2 (h_0 \sin\varphi \sin\delta + \cos\varphi \cos\delta \sin h_0),$$

where the solar declination angle δ and the Sun-Earth distance squared d^2 are strong (amplitude: about 0.4 rad = about 23º given by the latitude of a tropic or the obliquity of rotation axis) and week (corresponding to the small orbital eccentricity 0.0167) functions of seasonal cycle. These are related to the two extreme cases of planetary seasonal cycles (Fig. 4.4). The first category is typical in Uranus which has an obliquity as large as 82º, and generates a seasonal cycle of anti-phase between the both hemispheres (thus weaker and semiannual in the lower latitudes). Earth and Mars are also in this category, although Mars with a somewhat eccentric orbit[23] has partly of the second category. The second category generates a seasonal cycle of in-phase between the both hemispheres including the equatorial region, which is not major in our solar system (only in several comets and far outer "dwarf planets" if they have atmospheres) but may appear in now a few extrasolar planets (discovered since 1995). Venus with slow rotation

[23]This made Kepler discover the first/second of his planetary motion laws, and proved earlier astronomy (all true circle orbits) false.

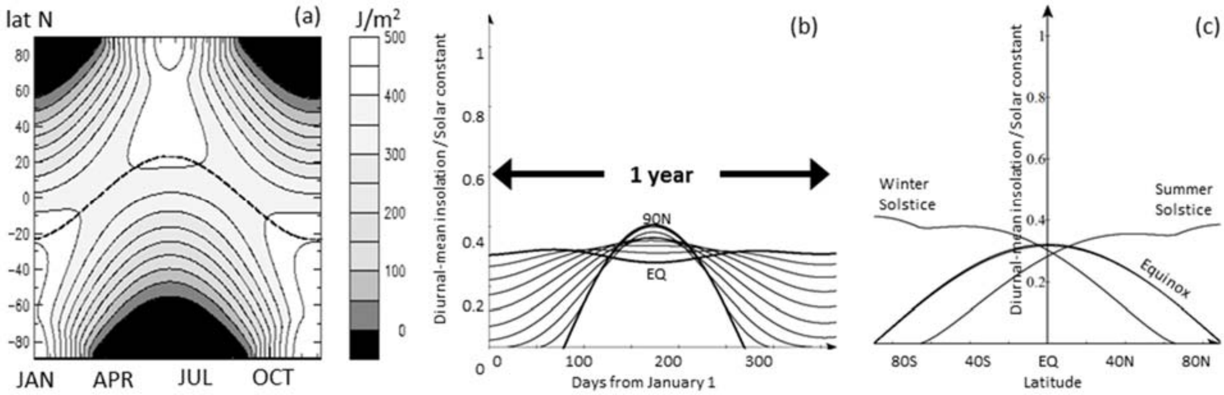

Fig. 4.5 (a) Seasonal-meridional, (b) seasonal and meridional variations of daily-mean insolation.

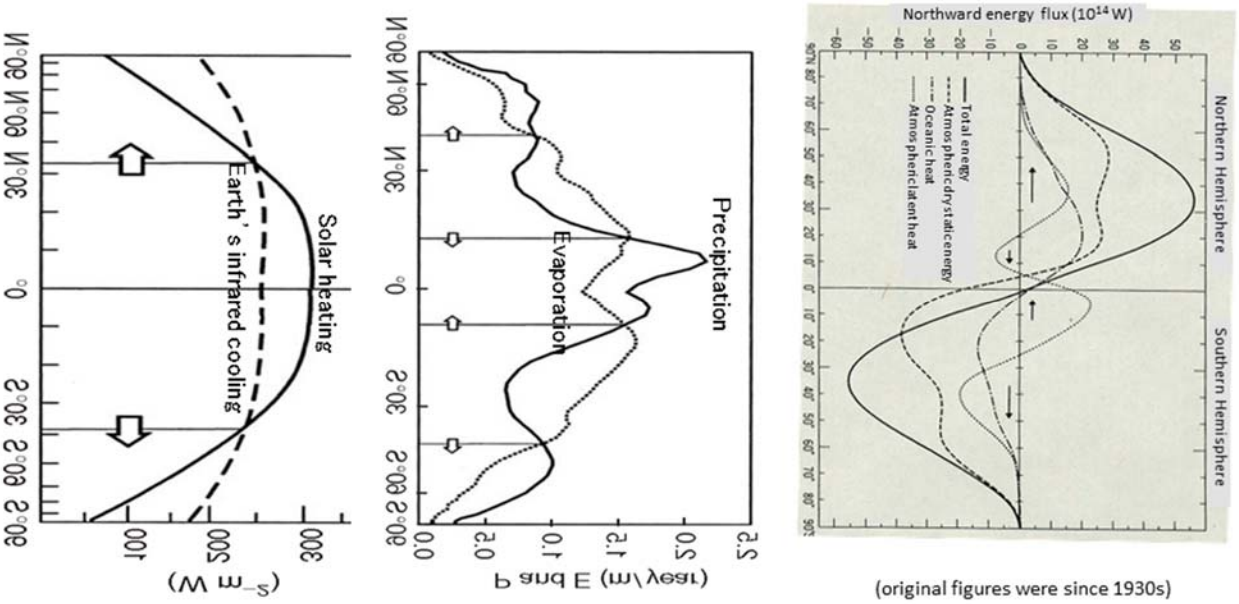

Fig. 4.6 Meridional distributions of radiative heat (left) and water (middle) budgets (Hartmann, 1994), and heat transports (right) (Palmen and Newton, 1969). Original data were from much older studies (since 1930s).

(probably due to strong tidal effect of Sun in a very close distance) and both very small eccentricity and obliquity has almost no seasonal/diurnal cycles.

The tropical specialty in meteorology/climatology such as the semiannual periodicity appears in the second category. Like this, temporal variability follows the astronomical formula relatively better, but meridional is not. It must be noted in Fig. 4.5 that the maxima of insolation appear in summer-hemispheric poles, and not in the tropics. This is consistent with an equatorially anti-symmetric temperature/wind distributions in the stratosphere (Fig. 4.2) and mesosphere (Section 4.4) mainly due to ozone absorption of the solar radiation (ultraviolet rays). However, by interactions with albedo or parasol effects (surface cryosphere and tropospheric clouds), the polar lower atmosphere lose much solar irradiance, and the tropospheric temperature/wind distribution is almost equatorially symmetric. In other words the meridional variability is more remarkable than temporal in the troposphere, and this is why the subfield of tropical meteorology/climatology is worthy to be studied.

When we integrate the solar heating for a year, we have the mean meridional distribution of insolation, which is approximately given by the equinoctial daily average except for the polar region:

$$\overline{Q}^{\text{year}} \dot{\propto} \overline{I_s}^{\text{year}} = \frac{1}{1\text{ year}}\int_0^{1\text{ year}} \overline{I_s}^{\text{day}}\, dt \approx \begin{cases} \left.\overline{I_s}^{\text{day}}\right|_{\delta=0} \approx \dfrac{I_{s0}}{\pi}\cos\varphi & \text{for } |\varphi| \le \delta_0 \\ \dfrac{I_{s0}}{\pi}\cdot(\text{daytime length}) & \text{for } |\varphi| \ge \delta_0 \end{cases}$$

where $\delta_0 = 23.4°$ is the obliquity angle. This corresponds to the sold curve in the left panel of Fig. 4.6. If this is balanced with the infrared radiation at any latitude as obtained as the vertical radiative-convective equilibrium (3.8),

$$\overline{T}(\varphi, p) = \left[\frac{I_{s0}}{2\pi\sigma}\left(\frac{\kappa}{g}p_0 + 1\right)\cos\varphi\right]^{1/4} \cdot \left(\frac{p}{p_{tp}}\right)^{\Gamma_c R/g} \quad \text{for } |\varphi| \le \delta_0 \text{ and } p > p_{tp}.$$

There may be zonal wind field with a vertical shear satisfying the thermal wind balance (4.11) or its L'Hospital form:

$$\frac{\partial\overline{u}}{\partial z} = -\frac{R}{fH}\frac{\partial\overline{T}}{\partial y} = -\frac{R}{faH}\frac{\partial\overline{T}}{\partial\varphi} = -\frac{R}{4faH\overline{T}^3}\frac{\partial\overline{T}^4}{\partial\varphi} = \frac{g}{8\Omega a\overline{T}^4}\frac{I_{s0}}{2\pi\sigma}\left(\frac{\kappa}{g}p_0 + 1\right)\left(\frac{p}{p_{tp}}\right)^{4\Gamma_c R/g} = \frac{g}{8\Omega a\cos\varphi},$$

or

$$\frac{\partial\overline{u}}{\partial z} = -\frac{R}{\beta H}\frac{\partial^2\overline{T}}{\partial y^2} = -\frac{R}{\beta a^2 H}\left(\frac{\partial^2\overline{T}}{\partial\varphi^2}\right) = -\frac{g}{8\Omega a\overline{T}^4}\left[\frac{\partial^2\overline{T}^4}{\partial\varphi^2} - \frac{3}{4\overline{T}^4}\left(\frac{\partial\overline{T}^4}{\partial\varphi}\right)^2\right] = \frac{g}{8\Omega a\cos\varphi}(1 + 3\tan^2\varphi),$$

which increases with latitude (the second term in the latter vanishes toward the equator $\varphi \to 0$). Quantitatively $g/8\Omega a = g/(8$ ·equatorial circumference/sidereal day) ≈$2.6\times10^{-3}\ \text{s}^{-1}$, or a westerly increase of 2.6 m/s per 1 km.

However, the actual temperature field is different from such a vertical one-dimensional equilibrium, and its meridional gradient rather smaller than the middle latitude is also not exactly balanced with the zonal wind which is also rather weak in average (Figs. 4.2 and 3). The tropical atmosphere is over-heated partly due to a hydrological cycle (only between atmosphere and ocean; cf. Webster, 1994) associated with a peak 2,000 mm/year of rainfall produced by clouds with spatially/temporally small scales which will be discussed in Chapter 6. Such an imbalance (shown between insolation and outgoing infrared radiation in the left panel of Fig. 4.6) must be compensated by meridional transport processes (shown in the right panel of Fig. 4.6) other than the geostrophic zonal flow, namely "ageostrophic" meridional circulations. They are associated with latent heat transport, which should be consistent with water budget (shown in the middle panel of Fig. 4.6). In the tropics or equatorial region overheating and over-precipitation are maintained by poleward heat transport and equatorial water vapor convergence[24]. Such meridional circulations will be dis cussed in the subsequent sections.

If the Earth is a completely even-surfaced sphere without interior activity, the liquid water as plenty as the actual Earth covers the whole Earth with a depth of 2,700 m, that is so-called an "aqua-planet" (right hand side panel of Fig. 4.7). Then the ocean as well as the atmosphere may flow zonally (as in stripe patterns of dense atmospheres of Jupiter and Saturn, and in the Earth's equatorial stratosphere as discussed in Section 5.4), if latitudinal differential heating (including that between summer and winter hemispheres) is adjusted almost geostrophically. However, Earth has the lands (about 3:7 to the oceans in area[25]) of which the eastern ends (coasts) turn equatorial easterly ocean currents

[24]For a solstice condition, i.e. including equatorially anti-phase seasonal variability, the equator plays a role of dehydrator on the way of energy/water transport from winter to summer.
[25]This land-sea area ratio has been conserved since at least 400 million years ago, in spite of their displacements by plate tectonics. Namely the liquid water amount and the solid Earth activity have been like that for such long years.

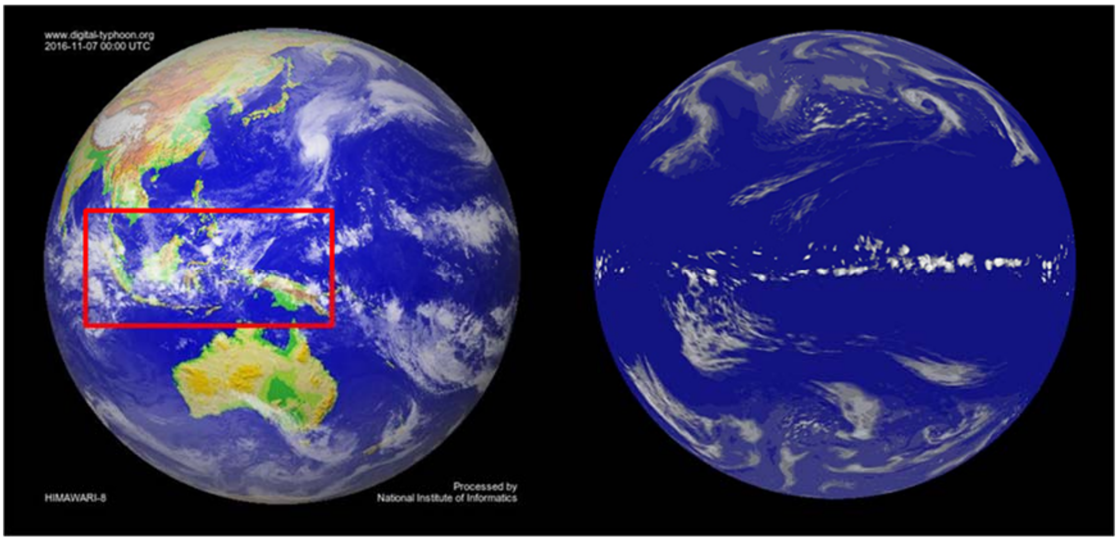

Fig. 4.7 Cloud distributions over the actual Earth observed by a meteorological satellite (left; an example at 00 UTC 7 November 2016; cf. Bessho et al., 2016; animations are obtained at http://agora.ex.nii.ac.jp/digital-typhoon/archive/monthly/index.html.en) and a virtual earth ("aqua-planet") with no lands simulated by a high-resolution numerical model (right; see Satoh et al., 2008; animations are obtained at http://www.jst.go.jp/kisoken/crest/ryoikiarchive/multi/en/theme/01_Sato.html). Tropical clouds over the actual Earth are rather different in particular on around lands (as indicated by a red rectangle in the left) from a zonally aligned structure over the aqua planet, although the actual and virtual middle/high-latitude clouds are almost similar (Yamanaka, 2016).

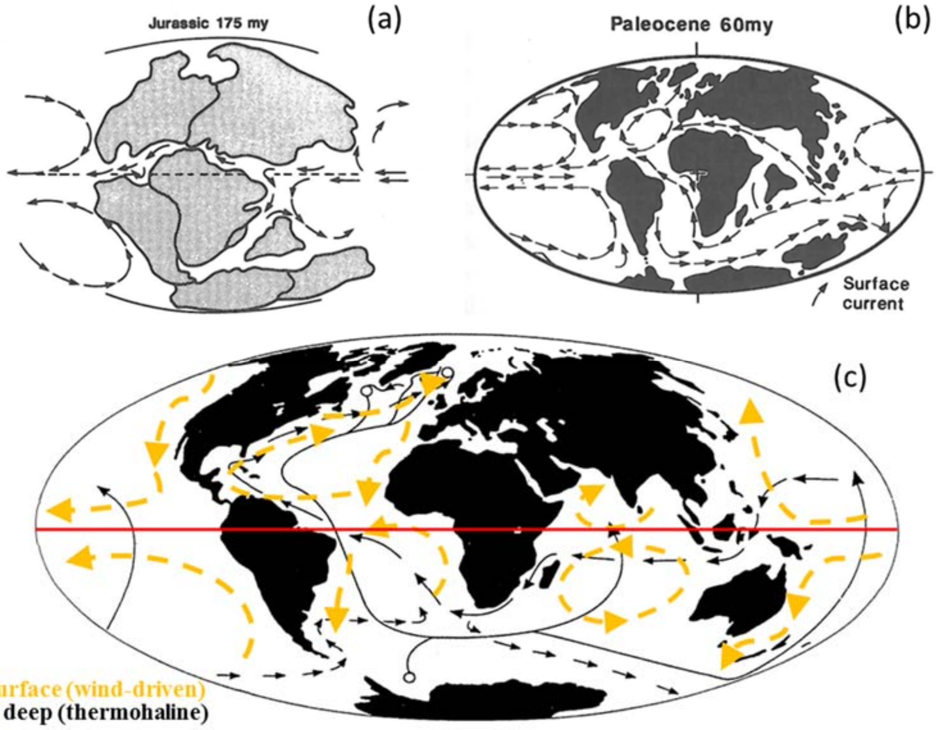

Fig. 4.8 (a) Mesozoic and (b) Cenozoic Tertiary continent distribution and ocean currents (Van Andel, 1994), compared with the present surface and deep ocean circulations (Bigg, 2003, with modification; originally from Prof. W. S. Broecker's idea proposed in 1987; see Broecker, 1991).

northward (such as Kuroshio and Gulfstream in the northern Pacific and Atlantic, respectively), although the ocean currents are almost zonal around the Antarctic continent and in the open oceans near the equator (Fig. 4.8), The coastal reflection of oceanic waves generates interannual variations (such as El Niño described in Section 5.3), and coastal contrast in heat capacity induces monsoon (Section 4.4) sea-land breeze (Section 6.1) circulations.

4.2. Potential vorticity conservation and inertial instability

Let us consider possibilities of co-existence or transience between the axi-symmetric zonal (easterly) flow discussed in the previous subsection and another axi-symmetric mode, that is, meridional circulations. Solving (4.2) and (4.6) for $\overline{v}$ and $\overline{w}$, we have

$$\overline{v} = \frac{-\left(\frac{\partial \overline{T}}{\partial z} + \Gamma\right)\left(\overline{G} - \frac{\partial \overline{u}}{\partial t}\right) + \frac{\partial \overline{u}}{\partial z}\left(\overline{Q} - \frac{\partial \overline{T}}{\partial t}\right)}{\rho_0 e^{-(R/C_pH)z} \cdot \overline{P}}, \quad \overline{w} = \frac{\frac{\partial \overline{T}}{\partial y}\left(\overline{G} - \frac{\partial \overline{u}}{\partial t}\right) - \left(\frac{\partial \overline{u}}{\partial y} - f\right)\left(\overline{Q} - \frac{\partial \overline{T}}{\partial t}\right)}{\rho_0 e^{-(R/C_pH)z} \cdot \overline{P}}, \tag{4.13}$$

where

$$\rho_0 e^{-(R/C_pH)z} \cdot \overline{P} = \frac{\partial \overline{u}}{\partial z}\frac{\partial \overline{T}}{\partial y} - \left(\frac{\partial \overline{u}}{\partial y} - f\right)\left(\frac{\partial \overline{T}}{\partial z} + \Gamma\right),$$

and

$$\overline{P} \equiv \frac{\overline{(\boldsymbol{\nabla}\times\boldsymbol{u} + \boldsymbol{f})}}{\rho_0} = \frac{1}{\rho_0}\left[\frac{\partial \overline{u}}{\partial z}\frac{\partial \overline{\theta}}{\partial y} + \left(f - \frac{\partial \overline{u}}{\partial y}\right)\frac{\partial \overline{\theta}}{\partial z}\right] = \frac{1}{\rho_0}\frac{\partial(\overline{\theta}, \overline{M}/a)}{\partial(y,z)}, \tag{4.14}$$

which is zonal-mean "Ertel's potential vorticity"[26] and

$$\frac{\partial(a,b)}{\partial(x,y)} \equiv \frac{\partial a}{\partial x}\frac{\partial b}{\partial y} - \frac{\partial a}{\partial y}\frac{\partial b}{\partial c}$$

is Jacobian.

Substituting (4.13) into (4.5), and replacing $\overline{u}$ and $\overline{T}$ by $\overline{\phi}$ from (4.3) – (4.4), we obtain the zonal-mean potential vorticity equation:

$$\rho_0\left(\frac{\partial}{\partial t} + \overline{v}\frac{\partial}{\partial y} + \overline{w}\frac{\partial}{\partial z}\right)\overline{P} = \frac{\partial(\overline{G}, \overline{\theta})}{\partial(y,z)} + \frac{\partial(e^{(R/C_pH)z} \cdot \overline{Q}, \overline{M}/a)}{\partial(y,z)}, \tag{4.15}$$

which implies that $\overline{P}$ must be conserved (for an air parcel) if there are no forcing ($\overline{G} = 0$, $\overline{Q} = 0$). In general such a Lagrangian conserved quantity may makes a field (being a function of space) if there is a force dependent on that quantity. In this case, if the parcel is displaced by any reason, there may be a difference between the parcel and the environment, and the force is also changed. If it is a restoring force, the parcel may be oscillating around the initial position, and it will return to the initial position if there are any decaying process such as friction or dissipation, which is called *stable*. On the contrary if the force enlarges the parcel - environment difference, the parcel never returns to the initial position, and the field will be modified (toward a new stable situation), which is called *unstable*.

In the present case an instability occurs if

$$f\overline{P} < 0 \quad \text{somewhere}, \tag{4.16}$$

which corresponds to the *inertial instability* in a rotating fluid: if inside is rotated faster than outside, a centrifugal force stronger inside than outside induces an instability[27] (cf. Andrews et al., 1987, Section 8.6). Substituting (4.13)

[26] Second-order nonlinear terms of disturbance quantities are omitted.

[27] When we include a viscosity, this instability is mathematically equivalent with the convective instability in section 6.2, and the Rayleigh number in the latter becomes the Taylor number with replacing the vertical temperature gradient $-N^2$ there by a vorticity product $f\overline{q}$ here (as shown below).

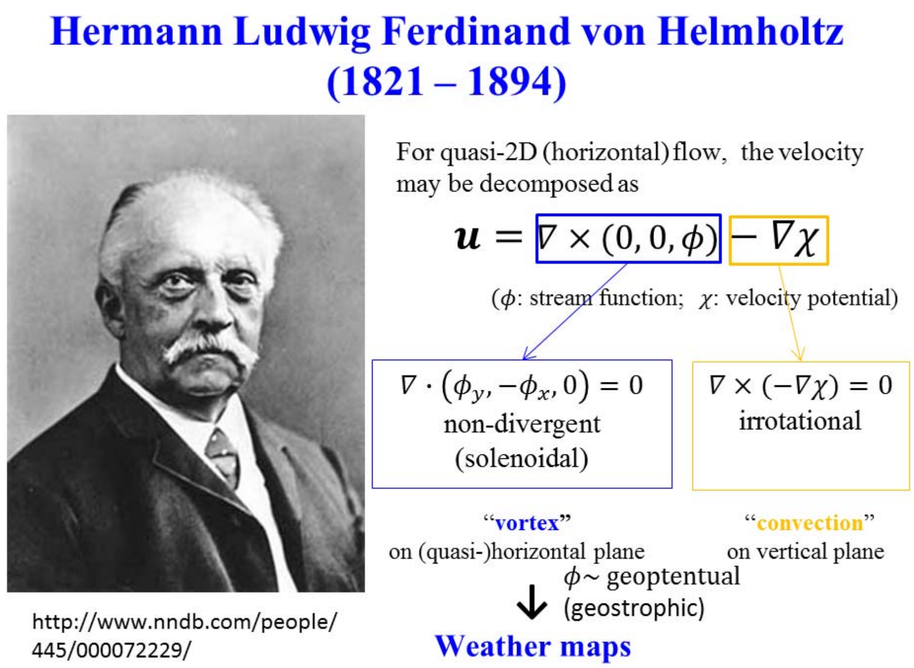

Fig. 4.9 One of many theorems derived by Helmholtz, concerning separation of fluid flow into non-divergent and irrotational components, which correspond to "vortex" in a horizontal plane and "convection" in a vertical plane. This separation is not unique. For the extratropics where the horizontal vortex motions are dominant a "weather map" is useful.

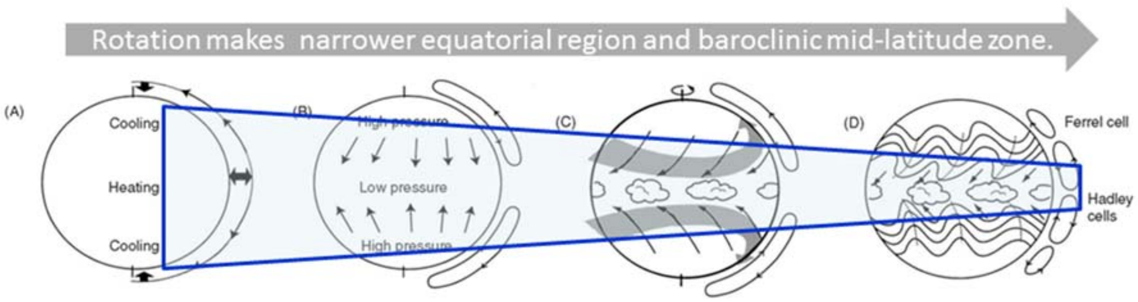

Fig. 4.10 Schematic depiction of the general circulation as it develops from a state of rest in a climate model for equinox conditions in the absence of land-sea contrasts of the equatorial region (where convective clouds controls circulation) (Wallace, 2002, with modification).

and (4.11), the condition (4.16) may be rewritten as

$$f\left[\bar{q}\frac{\partial\bar{\theta}}{\partial z} - f e^{(R/C_pH)z}\frac{H}{R}\left(\frac{\partial\bar{u}}{\partial z}\right)^2\right] < 0 \quad \text{somewhere},$$

that is,

$$Ri\left[f^2\left(1 - \frac{1}{Ri}\right) - f\frac{\partial\bar{u}}{\partial y}\right] < 0 \quad \text{somewhere}, \tag{4.17}$$

where

$$\bar{q} \equiv f - \frac{\partial\bar{u}}{\partial y} = \overline{f + \frac{\partial v}{\partial x} - \frac{\partial u}{\partial y}} = \overline{z \text{ component of absolute vorticity } f + \boldsymbol{\nabla}\times\boldsymbol{u}} \tag{4.18}$$

and

$$Ri \equiv N^2 \left(\frac{\partial \bar{u}}{\partial z}\right)^{-2} \ : \text{“Richardson number”},$$

$$N \equiv \left[e^{-(R/C_pH)z} \cdot \frac{R}{H}\frac{\partial \bar{\theta}}{\partial z}\right]^{\frac{1}{2}} = \left[\frac{R}{H}\left(\frac{\partial \bar{T}}{\partial z} + \Gamma\right)\right]^{\frac{1}{2}} \ : \text{“Väisälä − Brunt frequency”}. \tag{4.19}$$

The inequality (4.17) involves several types of instability:

$$Ri < 0 \ \ \text{(i.e., } N^2 < 0 \text{, or } \frac{\partial \bar{\theta}}{\partial z} < 0\text{)} \quad \text{“convective instability”;}$$

$$0 < Ri < \frac{f}{\bar{q}} \ \text{ and } \ f\bar{q} > 0 \quad \text{“symmetric instability”; and}$$

$$Ri \gg 1 \ \text{ and } \ f\bar{q} < 0 \quad \text{“inertial instability” (narrow meaning).}$$

These instabilities appear only in mesoscale or smaller phenomena near fronts in the extratropics, but are more important in the tropics where f is small and changes the sign (Dunkerton, 1981, 1983). Due to the inertial instability an axi-symmetric meridional circulation perpendicular to the axi-symmetric zonal flow may appear[28].

In general (by a theorem referred often to the name of Helmholtz; see Fig. 4.9) a geophysical fluid flow may be separated into a “vortex”-like component in a horizontal plane and a “convection”-like component in a vertical plane. The former is dominant when the rotation is increased (see Fig. 4.10). In the tropics with small f the “convection”-type motions including the meridional circulations (as well as a zonal-vertical circulation described in Section 5.2 and smaller-scale (narrow-meaning) convections discussed in Chapter 6) are dominant, and a “weather map” showing geopotential contours approximately recognized as geostrophic streamlines is useless.

4.3. Hadley circulation

The Hadley circulations were considered by an English lawyer George Hadley in the early 18th century, based on mariners' experience on the equatorial easterly (trade wind) drifting equatorward (cf. Section 7.1 of Lindzen, 1990; see later the top right panel of Fig. 4.12). Early thermodynamic studies at that time suggested also updraft near the equator with higher temperature, as a result of the buoyancy torque (Fig. 4.11(a)). However, the surface temperature maximum near the equator is not explained only by insolation intensity dependent on the solar zenith angle, because the daily-mean insolation takes a maximum in the summer pole without nighttime as appearing actually at the stratopause (see later Sections 4.5 and 5.4). The polar cooler surface climate is caused by larger reflection (cloud and cryospheric albedo, which is also a result of cooler climate, i.e., the ice-albedo feedback mechanism) and refraction (longer optical depth). As discussed in Section 3.2, if the one-dimensional radiative-convective equilibrium appears, zonal winds with no meridional circulation may appear under the thermal wind equilibrium. The vertical increase of westerly associated with poleward decrease of temperature under the thermal wind equilibrium may induce the Coriolis/centrifugal torque opposite to the buoyancy torque (Fig. 4.11(b)). Even if the stratification becomes unstable by local/instant stronger heating at the ground (as discussed in Section 6.2), such a convection should be ceased due to upward/outward heat transport by the convection itself. Therefore, to maintain

[28]Non-axisymmetric flows are waves to be described in Chapter 5.

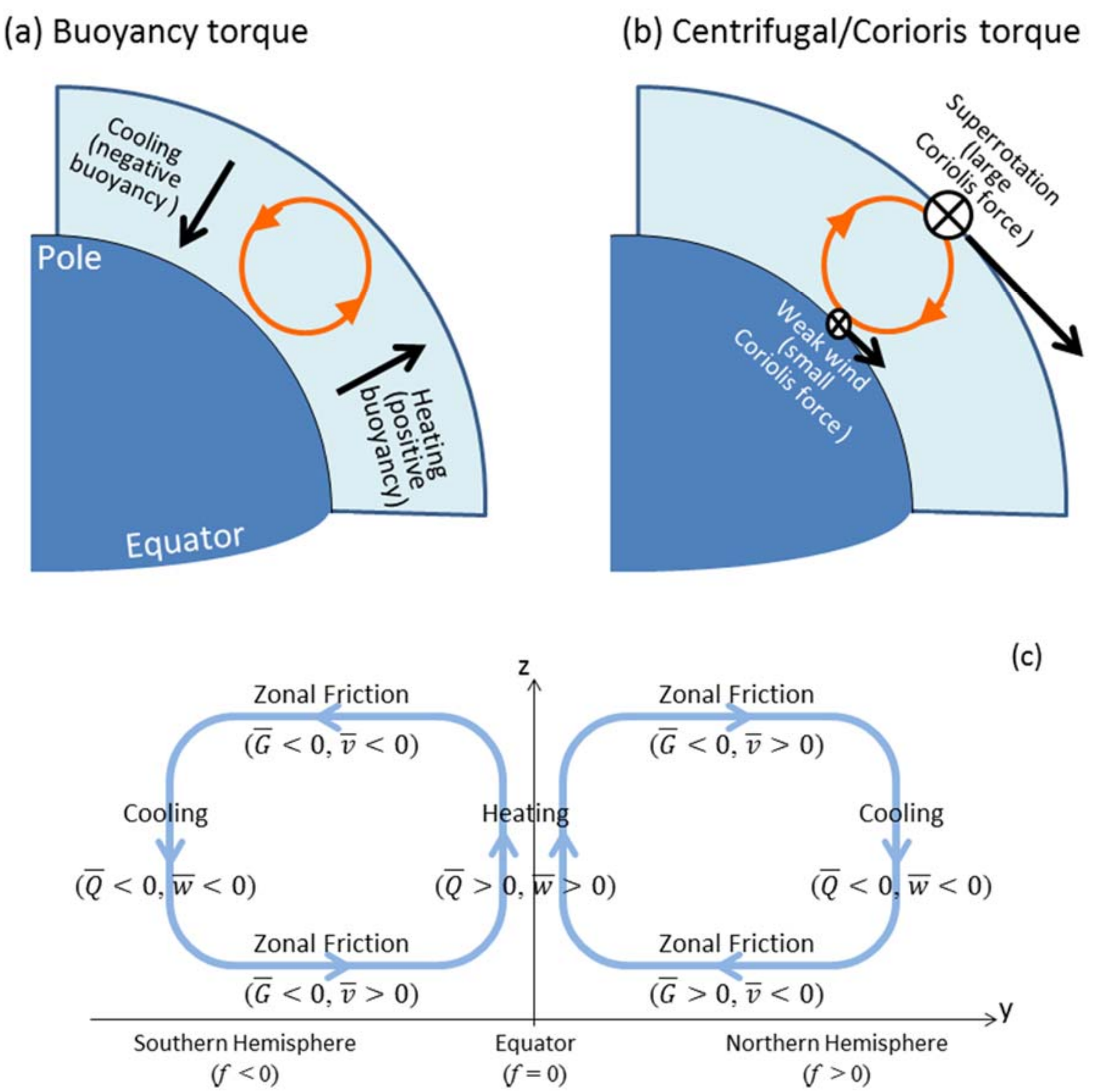

Fig. 4.11 Schematic figures of (a) heating and (b) shear torques working in the meridional plane (Matsuda and Yoden, 1985, with modification), and (c) the Hadley circulation forced by (a) (Holton, 1992, Section 10.2, with modification).

the Hadley circulation, any steady forcing is necessary both in the vertical and meridional directions to maintain the Hadley circulation.

Approximate forms of (4.13) and (4.16) (or (4.5)) for a steady ($\partial/\partial t = 0$) quasi-homogeneous ($\overline{u}$ and $\overline{T}$ almost constant) case are

$$\overline{v} \approx -\frac{\overline{G}}{f}, \quad \overline{w} \approx \frac{\overline{Q}}{\Gamma}, \quad \frac{\partial}{\partial y}\left(-\frac{\overline{G}}{f}\right) + \frac{1}{\rho_0}\frac{\partial}{\partial z}\left(\rho_0 \frac{\overline{Q}}{\Gamma}\right) \approx 0. \tag{4.20}$$

The first formula shows the so-called Ekman's relation that a *zonal* mechanical forcing $\overline{G}$ (such as a friction[29]) induces a *meridional* flow $\overline{v}$. The second formula shows that a net heating/cooling $\overline{Q}$ is canceled by an adiabatic

[29]A friction at the bottom is boundary layer turbulence (cf. Sections 6.1-2), which was noticed originally by Hadley and is observed actually as the trade-wind mixed layer (below an inversion layer) over open oceans. However, effects of local circulations with diurnal cycles near coastlines or on lands, as well as situations/mechanisms at the top of the Hadley cells (of which a possibility is due to any wave disturbances or their breaking; cf. Section 5.4) are still not completely clear.

cooling/heating (expansion/compression) through ascending/descending $\overline{w}$. The last diagnostic equation of (4.20) implies that the Hadley circulation must be generated so that both forcings $\overline{Q}$ and $\overline{G}$ are balanced.

If $\overline{Q}$ and $\overline{G}$ are expressed by $\overline{u}$ and $\overline{T}$ and/or their derivatives, so that they are damped (decrease in time), such as the Newtonian cooling (3.6), the Rayleigh damping (4.12) or the eddy diffusion (3.3), then the third equation of (4.20) and the thermal wind relation (4.11) are closed for two dependent variables $\overline{u}$ and $\overline{T}$. Alternatively, expressing $\overline{w}$ by $\overline{T}$, the continuity equation (4.5) (which is the original form of the third equation of (4.20)), the thermal wind relation (4.11) and the zonal momentum equation (4.2) (or (4.10)) are also closed for three variables $\overline{u}$, $\overline{v}$ and $\overline{T}$. The Hadley circulation with adiabatic cooling/warming (expansion/compression) induced by updraft/downdraft in the warmer/cooler side (lower/higher latitude) transports heat from the equator to the mid-latitudes, which makes the meridional temperature gradient $-\partial\overline{T}/\partial y$ smaller. Simultaneously, under the absolute angular momentum conservation (4.10), the Hadley circulation with poleward/equatorward flow in the upper/lower half decreases/increases the planetary angular momentum and increases/decreases the relative angular momentum (the westerly $\overline{u}$)[30], which increases the vertical shear $\partial\overline{u}/\partial z$. The Hadley circulation is generated so that modified $-\partial\overline{T}/\partial y$ and $\partial\overline{u}/\partial z$ satisfy the thermal wind relation.

When we assume equatorial symmetry ($\overline{v}=0$ at $y=0$), rigid top and bottom ($\overline{w}=0$ at $z=0,h$), vertical isentropic ($\overline{\theta}(y,z)=\overline{T}(y)$) and no zonal wind at the bottom ($\overline{u}=0$ at $z=0$), we integrate the thermal-wind relation (4.11) meridionally (from 0 to y) for a zonal wind field $\overline{u}=\beta y^2/2$ which conserves the absolute angular momentum conservation (4.8) at the top ($z=h$), and obtain

$$\frac{\overline{T}(0)-\overline{T}(y)}{T_0}=\frac{y^4}{8\lambda^4},\quad \lambda\equiv\left(\frac{gh}{\beta^2}\right)^{1/4}\quad \text{"equatorial radius of deformation"}, \tag{4.21}$$

where T_0 is a representative value of temperature used for calculation of the scale height H. The most important parameter λ corresponds to the Rossby's deformation radius in mid latitudes, which is defined by the gravity wave phase velocity divided by f (see Section 5.1). Held and Hou (1980) considered that the Hadley circulation is generated within a latitude range $|y|\leq$, so as to cancel the net difference (negative/positive in the equatorial / mid-latitudinal sides) between temperature $\overline{T}(y)$ modified by the circulation and the radiatively equilibrated temperature $T_e\equiv T_0(1-\Delta\cdot y^2/a^2)$:

$$\int_0^Y \overline{Q}(y)\,dy=-\alpha\int_0^Y\left[\overline{T}(y)-\overline{T}_e(y)\right]dy=0,\quad \overline{T}(Y)=\overline{T}_e(Y),$$

which gives the meridional width Y of the Hadley circulation as

$$\frac{Y}{a}=\left(\frac{5}{3}\Delta\frac{4\lambda^4}{a^4}\right)^{1/2}\sim 0.3.$$

Lindzen and Hou (1988) explained seasonal-meridional variations of the Hadley circulation by equatorially-asymmetric heating.

More exact solutions: (which is equivalent to "zero zonal wavenumber" case of equatorial waves; cf. Chapter 5) may be obtained, as long as the atmosphere is assumed approximately to be incompressible (4.5) and in the

[30]This "superrotation" mechanism increases also the total rotation speed by decreasing the rotating radius, as done by a figure skater who cannot go out of a narrow skating rink without variations of the planetary angular momentum but can decrease the rotating radius drastically.

thermal-wind (hydrostatic-geostrophic) equilibrium (4.11). If we use a zonal-mean meridional stream function $\overline{\psi}$ satisfying (4.5):

$$\overline{v} = -\frac{1}{\rho_0}\frac{\partial\overline{\psi}}{\partial z}\,, \quad \overline{w} = \frac{1}{\rho_0}\frac{\partial\overline{\psi}}{\partial y}, \tag{4.22}$$

we obtain $\partial(4.6)/\partial y - \partial(4.2)/\partial z$ as a 'diagnostic' equation[31] concerning only one dependent variable $\overline{\psi}$:

$$\frac{\partial^2\overline{\psi}}{\partial y^2} + \frac{f^2}{N^2}\rho_0\frac{\partial}{\partial z}\left(\frac{1}{\rho_0}\frac{\partial\overline{\psi}}{\partial z}\right) = \frac{\rho_0}{N^2}\left[\frac{\partial}{\partial y}\left(\frac{R}{H}\overline{Q}\right) + f\frac{\partial\overline{G}}{\partial z}\right], \tag{4.23}$$

which is of the elliptic (or Poisson's) type, and takes a solution in a region where the external forcing $\overline{Q}$ and/or $\overline{G}$. For simplicity here we sketch only a fundamental solution for an equinox (equatorially symmetric) situation, with the zenith angle of solar culmination (the maximum insolation incident angle) given by the latitude φ (see Sections 4.1, 4.4 and 6.1). Then the insolation is proportional to $\cos\varphi$, and simplified appropriate forms of the forcing terms and the righthand-side of (4.23) are

$$\overline{Q}(y,z) \dot{\propto} \cos ly \sin mz, \qquad \overline{G}(y,z) \dot{\propto} \sin ly \cos mz, \quad i.e., \ \text{RHS of (4.23)} \dot{\propto} -\sin ly \sin mz$$

in the domain $-\pi/l < y < \pi/l\,,\ 0 < z < \pi/m$. Thus the solution of (4.23) should be

$$\overline{\psi} \dot{\propto} -\sin ly \sin mz, \quad i.e. \quad \overline{v} \dot{\propto} -\sin ly \cos mz, \qquad \overline{w} \dot{\propto} \cos ly \sin mz,$$

which corresponds to a pair of meridional circulation cells in the northern/southern sides of the equator.

The forcing terms $\overline{Q}$ and $\overline{G}$ involve also nonlinear products of perturbed quantities defined as $(\quad)'$ in (4.1). Such perturbation quantities may have systematic structures (such as phase and polarization relationships for a wave to be described in Chapters 5 and 6), and their nonlinear products may not always induce a 'thermally direct' motion (upward/downward in the warmer/cooler sides) as the Hadley circulation. For example, a baroclinic (external Rossby) wave in the mid-latitude westerly has an indirect (Ferrel) circulation (downward/upward in the warmer/cooler sides). In the lower stratosphere a mechanical forcing $\overline{G}$ (divergence of momentum flux) of upward propagating waves induce an indirect meridional circulation in higher latitudes (Section 4.5), and quasi-periodic (quasi biennial and semiannual) variations of mean zonal wind $\overline{u}$ near the equator (Section 5.4).

It is rather simple in a two-dimensional (zonal-mean) problem as mentioned above that a meridionally differential heating (temperature gradient) $\overline{Q}$ and its balance (4.20) with mechanical forcing (friction) $\overline{G}$ may induce/maintain the Hadley circulation. However, in a more realistic three-dimensional problem, there may be possibilities to generate axi-assymetric (zonally wavy) disturbances (which will be discussed in Chapters 5 and 6). It is important that near the equator the Coriolis force vanishes and thermally indirect circulations (with Rossby and baroclinic waves) are too weak to cancel the Hadley circulation. Furthermore, in spite of the horizontally uniform heating at the bottom (and conditionally unstable stratification as mentioned in Sections 3.3. and 6.2), smaller-scale vertical (Benárd-Rayleigh) convections are not so superior as to destroy the Hadley circulation and its updraft zone ITCZ, which (as well as a zonal circulation described in Section 5.2) will be explained by cloud-convection organization activities of waves trapped near the equator with not negligible meridional gradient (the β-effect) of the

[31] In the weather prediction an equation without the time derivative (that is, not necessary to be integrated in time) is called as a medical word 'diagnostic', and in particular one equivalent to (4.23) as 'Omega equation' because it gives the 'vertical velocity' ω mentioned in the footnote of Section 3.4. (4.23) is also mathematically similar to an equation for convections (Chapter 6), but is physically different from the latter because (4.23) needs Earth's rotation f and mechanical forcing (friction) G.

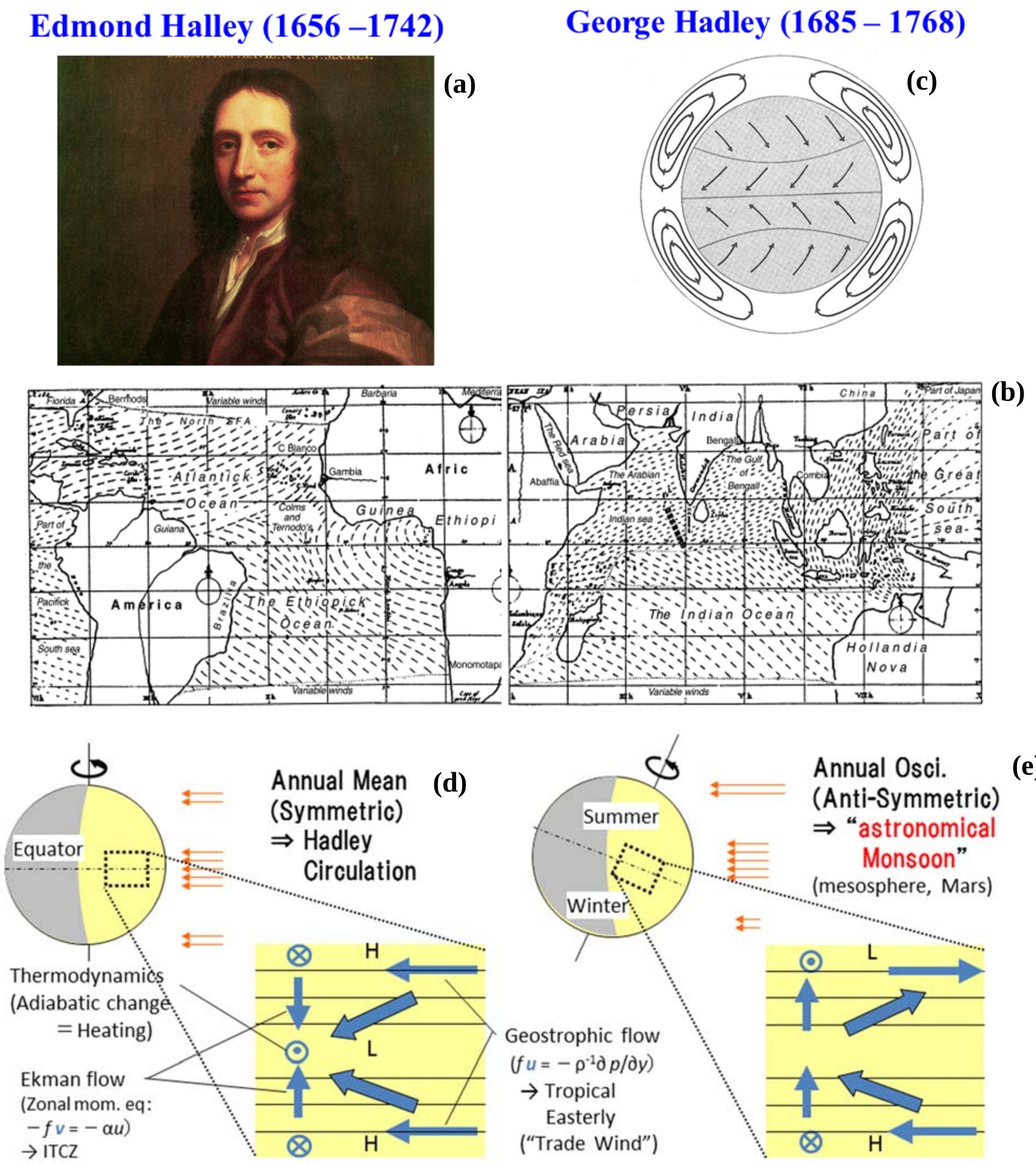

Fig. 4.12 (a) British astronomer Halley and his (b) historically first (1686) wind distribution map, on which (c) Hadley's (1785) circulation theory was based. Hadley plotted only wind directions including both (d) the Hadley circulation and (e) monsoon, which can be explained by Hadley who first included Earth's rotation (later called the Coriolis force).

Coriolis force. More precisely speaking, ITCZ is not located just at the equator, and its annual north-southward shift is not symmetric (rather to the north). Double ITCZ-like features are found around the Indonesian maritime continent (IMC), including a less clear convective-cloud band extended east-southeastward from IMC in the southern Pacific (the south-Pacific convergence zone, or SPCZ). These features have been considered at first due to sea surface temperature (SST) distributions resulted from interannually variated interactions with ocean (Section 5. 3), such as suppression of convective activities due to 'equatorial upwelling' of cooler deep water associated with 'Ekman friction' of surface trade wind. A double ITCZ was obtained also in the initial 'aqua-planet' numerical experiment

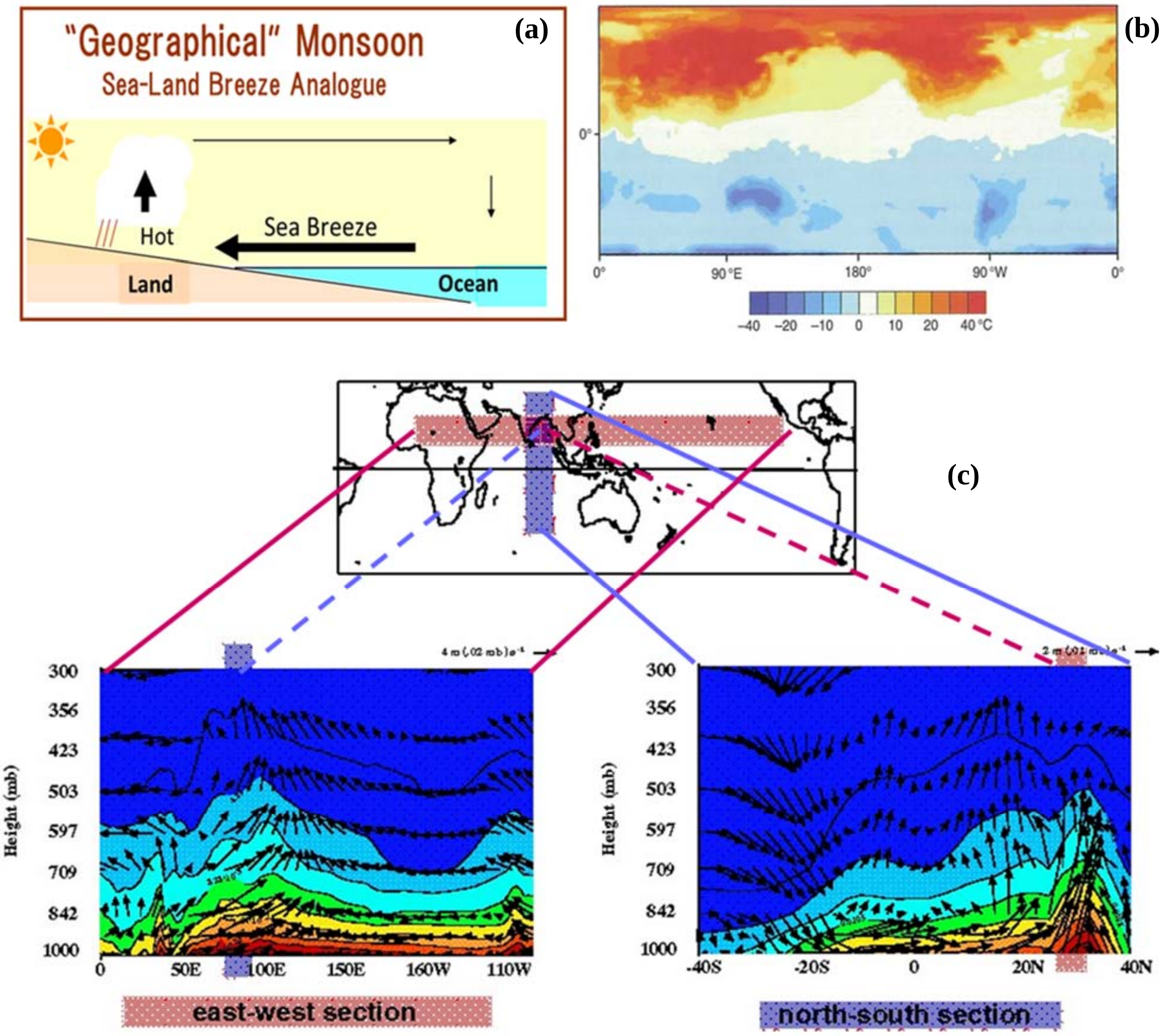

Fig. 4.13 (a) Schematic figure of 'geographical' monsoon, (b) the "Find the Continents" game, by July minus January surface air temperature (Wallace and Hobbs, 2006), and (c) zonal and meridional circulations in the northern summer monsoon season (Webster et al., 2002).

by a perpetual equatorially-symmetric SST model (Hayashi and Sumi, 1985), and it (or broader ITCZ) is considered due to weaker moisture convergence associated with weaker Hadley circulation (Numaguti, 1993).

4.4. Monsoon circulation

Human beings recognized and utilized the annual cycle of climate since Mesopotamia-Indus trades at least 4,000 years ago. In 45 BC Caesar established the Julian calendar based on a solar year, and summarized the seasonal reversals of wind known by Orient and Greek sailors which later called *mausim* by Arabic mercantile mariners over the Indian Ocean. From the opposite side Indonesian people immigrated Madagascar many times, and a great Chinese-Muslim voyager Zheng He (Cheng Ho) sailed to Africa in early 15th century. Again from west European Age of Discovery/Exploration in 15-17th centuries was based on the knowledges of the monsoon, which were plotted in Halley's (1686) global map of ocean surface wind (Fig. 4.1(c)). In 19-20th centuries, based on surface meteorological observations extended globally, modern geographical climate classifications were proposed. The first one by a German climatologist Köppen was based on monthly-mean (annually-cycling) temperature and precipitation, and major types were named with characteristic vegetations, such as rainforest (symbol: *Af*) and savanna (*As*) in the tropical climate (*A*). An intermediate type (*Am*) between *Af* and *As* classified by Köppen was later re-defined and called as the tropical monsoon climate. In 1950s a Russian climatologist Khromov showed a global distribution of monsoon defined as January-July wind azimuth difference larger than 120º, from which Ramage (1971) of Hawaii restricted only such regions in tropical Asia and Africa by omitting wind rotations due to extratropical cyclones, as well as weak wind inside of the subtropical anticyclone zone. In the Asian monsoon region monsoon from/beyond ocean is associated with active rainfall, and monsoon is often identified with the rainy season (Murakami and Matsumoto, 1994; Wang and Ho, 2002).

The insolation has a hemispheric anti-phase annual cycle associated with the revolution of Earth with inclined rotation axis (as described in Section 4.1). On a solstice day the daily mean insolation $\overline{I_s}^{\mathrm{day}}$ at the summer-hemispheric tropic line is about twice of that at the winter-hemispheric one, which produces upward/downward buoyancy torques in the summer/winter hemispheres. The meridional temperature gradient also generates the vertical shear of geostrophic (thermal-wind-equilibrated) zonal flow (Section 4.1), and the buoyancy torque may be reduced by the vertical shear torque. However, a friction working on the zonal flow enforces an *a*geostrophic meridional flow so as to be balanced with the Coriolis force in latitudes apart from the equator. By these processes for the northern-hemispheric summer solstice

$$\overline{Q}(y,z) \dot{\propto} \sin ly \sin mz, \qquad \overline{G}(y,z) \dot{\propto} -\cos ly \cos mz, \quad i.e., \quad \text{RHS of (4.23)} \dot{\propto} -\cos ly \sin mz$$

in the domain $-\pi/l < y < \pi/l$, $0 < z < \pi/m$, and hence the solution of (4.23) should be

$$\overline{\psi} \dot{\propto} -\cos ly \sin mz, \quad i.e. \quad \overline{v} \dot{\propto} \cos ly \cos mz, \qquad \overline{w} \dot{\propto} \sin ly \sin mz,$$

which corresponds to a globally one-cell meridional circulation (Fig. 4.12(e)). For the northern-hemispheric winter solstice, these quantities have opposite signs, so that the circulation becomes reversed. Because of this 'astronomical' monsoon circulation, the in-phase winter-hemispheric Hadley cell is always larger and stronger than the anti-phase summer-hemispheric cell. Other examples of this type of monsoon are the general circulations of Earth's middle atmosphere and Matian atmosphere.

In addition the insolation on Earth produces another buoyancy torque between land and sea surfaces, which enforces another category of annually reversed circulation (say, 'geographical' monsoon) of the free troposphere (Fig. 4.13). In the first law of thermodynamics for an almost incompressible body (liquid and solid) the expansion work (which is quite important for gas; cf. Chapter 2) is negligible, and the temperature increase for a heating is almost inversely proportional to the heat capacity of the body. For insolation on Earth's surface, the solid land surface (more exactly a thin layer of soil) with a smaller heat capacity (about 1/5) has a higher temperature much smaller than the liquid sea surface. Heat conduction in a solid and diffusion in a liquid are not so simple, but in the actual seawater with sufficiently large size and depth eddy diffusion may make the surface/local heat escape to deeper/surrounding water, which contribute to sufficiently smaller/slower response of the sea surface temperature than the land surface temperature. Although atmospheric radiation and response are more complex than sea or land surfaces, such as albedo dependent on the land surface feature (including vegetation which also has seasonal variations called phenology) and various boundary layer processes (cf. Section 6.1), the lowest atmosphere follows the bottom surface temperature

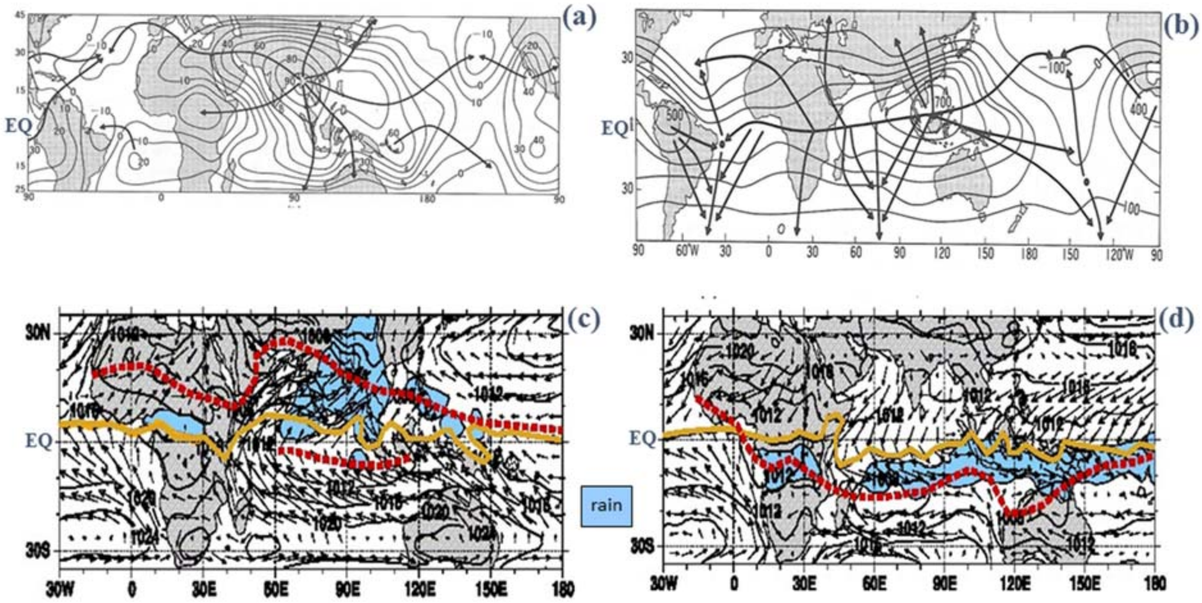

Fig. 4.14 (a)(b) Upper-tropospheric (200 hPa) velocity potential and divergence (Krishnamulti et al., 1973; Krishnamulti, 1971), and (c)(d) lower-tropospheric (925 hPa) wind and rainfall (Webster, 1999) for boreal (a)(c) summer (June-August) and (b)(d) winter (December-February) (Webster et al., 2002).

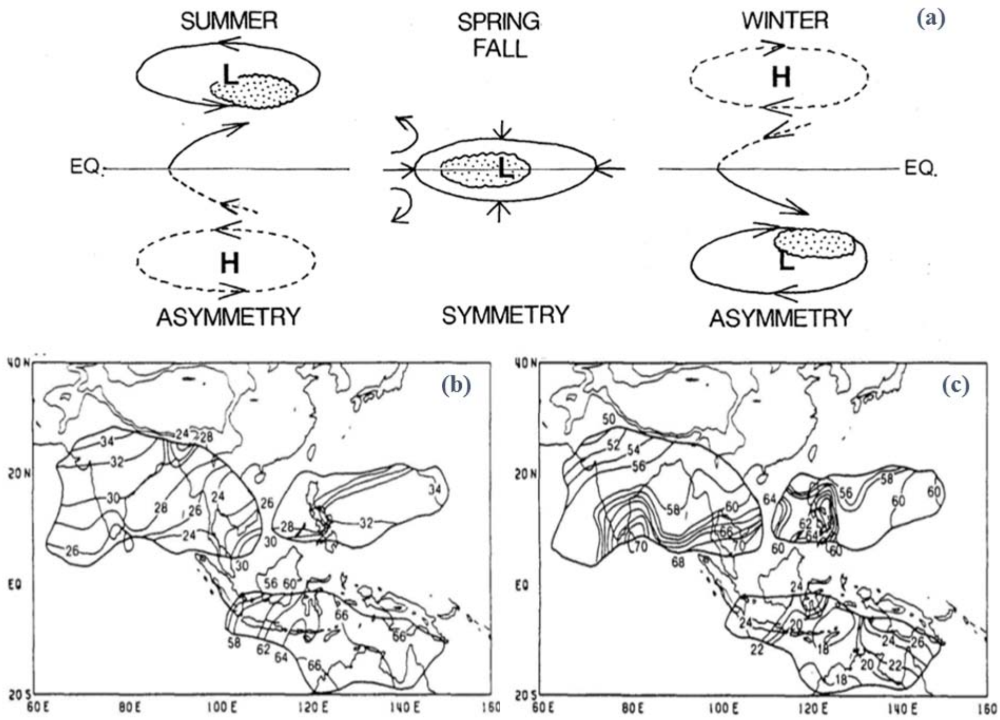

Fig. 4.15 (a) Seasonal cycle of the ITCZ location indicated by dotted area (Matsumoto and Murakami, 2000), and rainy-season (b) onset and (c) withdrawal isochrones indicated by pentad number (Murakami and Matsumoto, 1994).

with a time lag, and the air temperature on a continent-scale land surface becomes warmer than on ocean-scale sea surface in summer with maximum annual-cycle insolation. In winter nighttime the lower continental atmosphere is cooled down more largely and quickly than the lower marine atmosphere.

These two categories of monsoon correspond to atmospheric tides (see Section 5.1) and sea-land breeze circulations (Section 6.1) for the diurnal cycle of insolation associated with Earth's rotation. The atmospheric tides

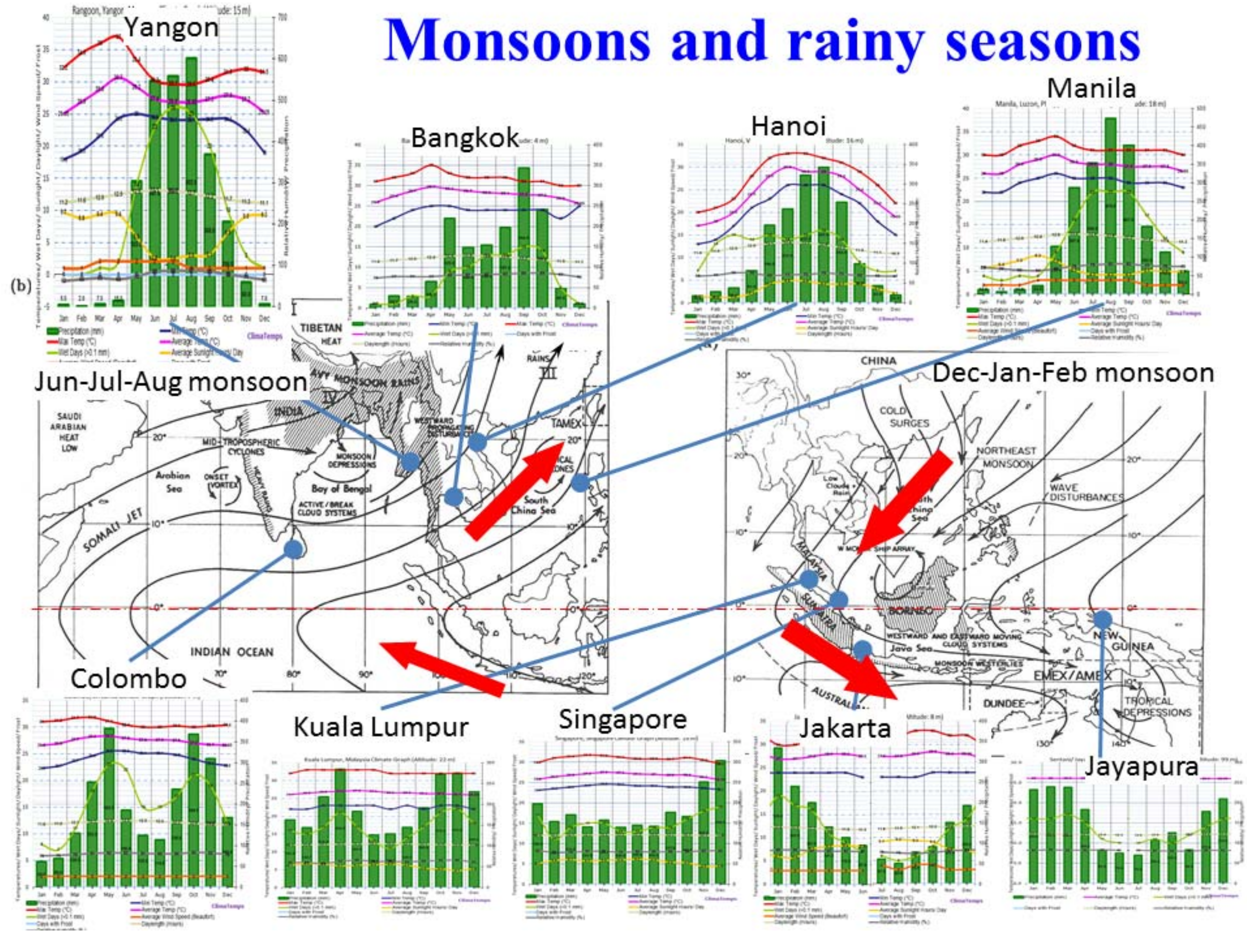

Fig. 4.16 Boreal summer and winter monsoons (Johnson, 1992) and annual rainfall cycles.

have global phase structures, enforced by a buoyancy torques between the day- and night-side hemispheres. The sea-land breeze circulations have local structure along a coastline. In the wave dynamics (Chapter 5) the equator and a coastline have a similarity as wave guides (having each trapped modes), but the double-digit magnitude difference (of 365 times) between Earth's revolution and rotation periods leads to differences of types of forced motions. Anyway Earth's troposphere is strongly affected by surface inhomogeneities such as sea-land distribution and land topography, and the 'geographic' monsoon (and sea-land breeze circulation) is relatively dominant in comparison to the 'astronomical' monsoon (and tides). However, in the Earth's middle atmosphere (cf. Section 4.5) and in the Martian atmosphere the 'astronomical' monsoon is dominant, which makes annually reversed meridional circulations.

In the atmosphere an upward motion associated forced by the buoyancy torque may generate a cloud (Section 6.2), and in the cloud the upward motion is enhanced by the latent heat released by cloud condensation itself. In this meaning a summer 'geographical' monsoon blowing from the ocean may have richer moisture and more intense cloud activity than a winter 'geographical' monsoon from the continent, and these monsoon periods are called rainy (or wet) and dry seasons (see Fig. 4.16). This makes often 'geographical' monsoons more remarkable than 'astronomical' monsoons.

In the Indian Ocean sector with continent and ocean distributed respectively in the northern and southern hemisphere, both the two mechanisms may work, and the most typical monsoon climate appears. This is why the

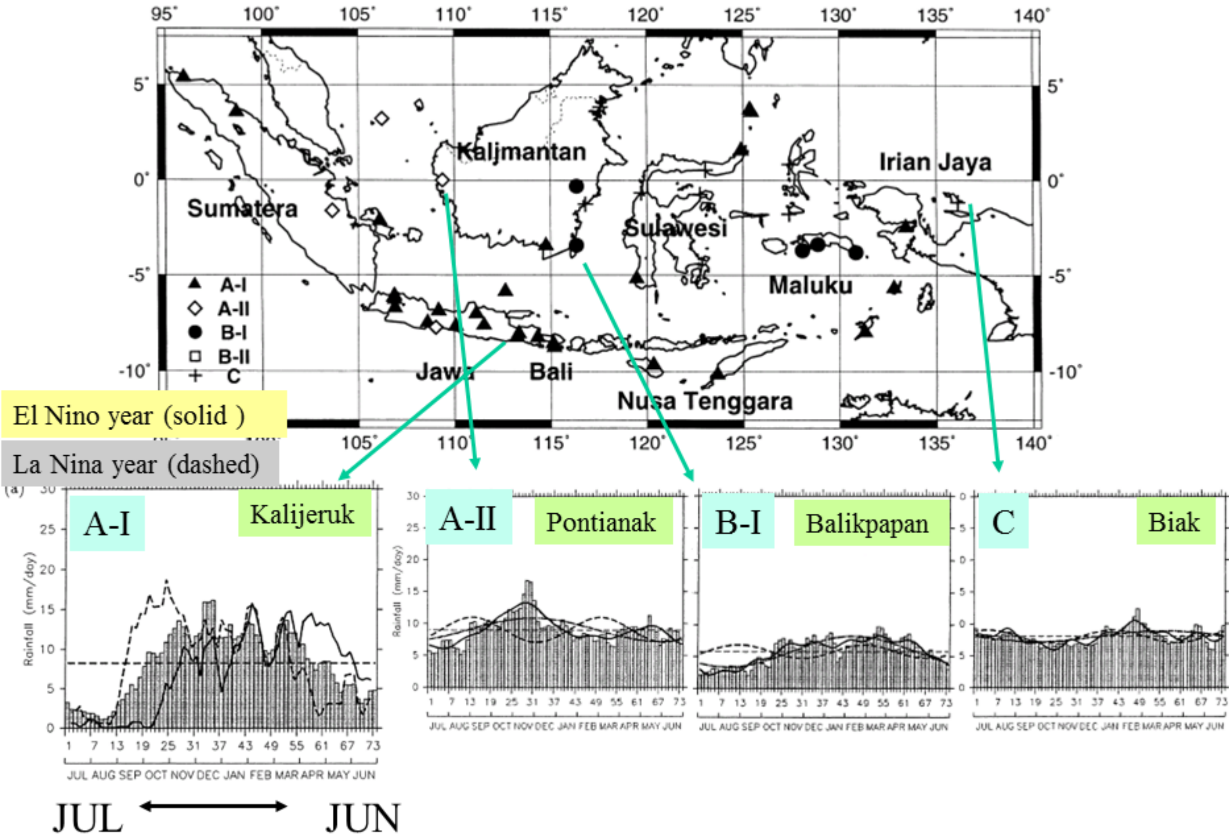

Fig. 4.17 Pentad-mean rainfall variations averaged for all (bars), El Niño (solid) and La Niña (dashed) years at typical stations, compared with each mean pentad rainfall (horizontal dashed line) (Hamada et al., 2002).

Arabs noted, utilized and named monsoon from long ago. In Japan a winter 'geographical' monsoon from the east Eurasian (Siberian) continent absorbs moisture from a warm water of the Sea of Japan and brings heavy snowfalls, This northern winter monsoon may blow beyond the equator (as an 'astronomical' monsoon; often called 'cold surge') with absorbing massive moisture over the East and South China Sea, and may produce strong southern summer monsoon and heavy rainfalls in the southern hemispheric side of the Indonesian maritime continent.

Eurasia, the largest continent with Himalaya-Tibet as the world's ceiling, generates a remarkable heat contrast with the Pacific and Indian Oceans, which enforces the most extensive monsoon circulation, the Asia monsoon (Fig. 4.14). A divergent wind (net air mass outflow) due to pressure gradient force at the upper levels is directed from over the continent with larger tropospheric (say, 1000-200-hPa) thickness (higher temperature) to over the ocean, which generates a thermal low over the continental surface and a convergent wind at low levels. This low-level flow makes convergences of not only air mass (to compensate the upper outflow) but also moisture, which makes so-called conditional instability (Section 6.2) in the boundary layer to develops cumulus convection. The monsoon circulation driven mainly by this mechanism is originally *a*geostrophic, but cyclonic/anticyclonic vorticities accumulated at the lower/upper levels generate geostrophic flow over around the continent, because the latitudes are so high that the Coriolis force works. For monsoon (4.20) holds approximately, and the vertical motion is almost positively correlated with temperature field[32]. Monsoons are made stronger and taller (almost throughout the troposphere) as observed,

[32]Energetically, the 'geographical' monsoon converts a potential energy generated locally (as an 'eddy' part defined in the midlatitude dynamics where the zonal-mean field is dominant) by diabatic (radiative and latent) heating, to kinetic energy dissipated frictionally at last. (See, e.g., Holton, 1992, Section 11.1.4.)

due to the latent heat released by clouds and precipitation over the continent in summer and over the ocean in winter.

In the northern-hemispheric summer the Eurasian continent is overheated by insolation in comparison to the Indian and Pacific Oceans. In particular the heating, surface pressure reduction and updraft over the Tibetan Plateau is very strong, which enforces strong warm and moist flow from the Indian Ocean to the southern slope of the Himalaya Mountains (cf. Fig. 4.14) and brings the rainy season of the Indian subcontinent. The rainy season is started from inland areas in the northeastern India and the Indochina peninsula (Matsumoto, 1992). The latter is continued to the lower mid-latitude eastern Asia (Chinese *Mei-yu*, Korean *Chang-ma*, and Japanese *Bai-u*), which are characterized by tropics-like cloud-cluster rainfalls[33] but are regarded as features of transient sub-season before the mid-summer covered by the subtropical (Pacific) anticyclone zone. Such seasonal marches can be seen clearly in the satellite observations (*e.g.*, Matsumoto and Murakami, 2000). In the onset of monsoon and rainy season the tropospheric vertical structure is also changed, and in the inland area of Indochina peninsula ascending of an inversion layer determining the convective cloud top is observed (Nodzu et al., 2006). The onset of monsoon and rainy season is often abruptly, and rainfall is quite inhomogeneous in space and time due to superimpositions of diurnal and intraseasonal variations near the equator (see Sections 6.1 and 6.4) and tropical cyclones in the subtropics (Section 6.3). Furthermore, the rainy-season duration and total rainfall amount have remarkable interannual variability (see Section 5.3).

In the northern-hemispheric winter cooled atmosphere on the Himalaya Mountains flows down toward the Indian Ocean, and the Indian subcontinent has a wintertime drought (cf, Fig. 4.14). Similar outflow (called *cold surge*) from the northeastern central Eurasian continent (Siberia) blows over Korea, Japan and China, and goes through the East and South China Seas to the southeast Asia. Extremely strong cold surges often go beyond the equator, and cause torrential rainfalls even in the southern-hemispheric part of the Indonesian maritime continent.

In the Indonesian maritime continent locating between Eurasian and Australian continents to the north and south, the both boreal and austral summer monsoons associated with the annual-meridional shift of the ITCZ are very clear (Figs. 4.15 and 4.17), which is also seen as the stronger/larger winter-hemispheric Hadley cell, as have mentioned already. Because of this basic behavior of the ITCZ and monsoon, the rainy season over the maritime continent differs/moves meridionally, and thus the maritime continent may be divided into roughly three climatic regions on the both sides and vicinity of the equator with austral/boreal summer single peak and with semiannual double or unclear peaks, respectively (*e.g.*, Schmidt and Ferguson, 1951; Murakami and Matsumoto, 1994; Hamada et al., 2002; Hendon, 2003; Aldrian and Susanto, 2003; Chang et al., 2004b, 2005) . More precisely there are two onset migration routes of the austral summer rainy season (Murakami and Matsumoto, 1994): one starts from the Indian Ocean side of Jawa in the middle September, and propagates northward (in Jawa) and eastward (to Nusa Tenggara in middle December); the other one is from Papua to Nusa Tenggara (Lesser Sunda Islands from Timor to Bali). The withdrawal of the austral-type rainy season starts from western Nusa Tenggara in March, and goes eastward (to eastern Nusa Tenggara), and westward (to Jawa), until late May.

However, because there are two geographical (equatorially asymmetric continent-ocean placement and steep mountain topography) and two spectral reasons (dominant interannual and intraseasonal variations), the annual cycle

[33] A major difference from the real (equatorial) tropics is that the cloud clusters are organized in (medium-scale, or meso-β-scale) extratropical cyclones (because of the Coriolis force) on a stationary front. In Japan another similar sub-season (*Shu-rin* or *Aki-same*) appears also after the mid-summer, and often associated with typhoons (see Section 6.3).

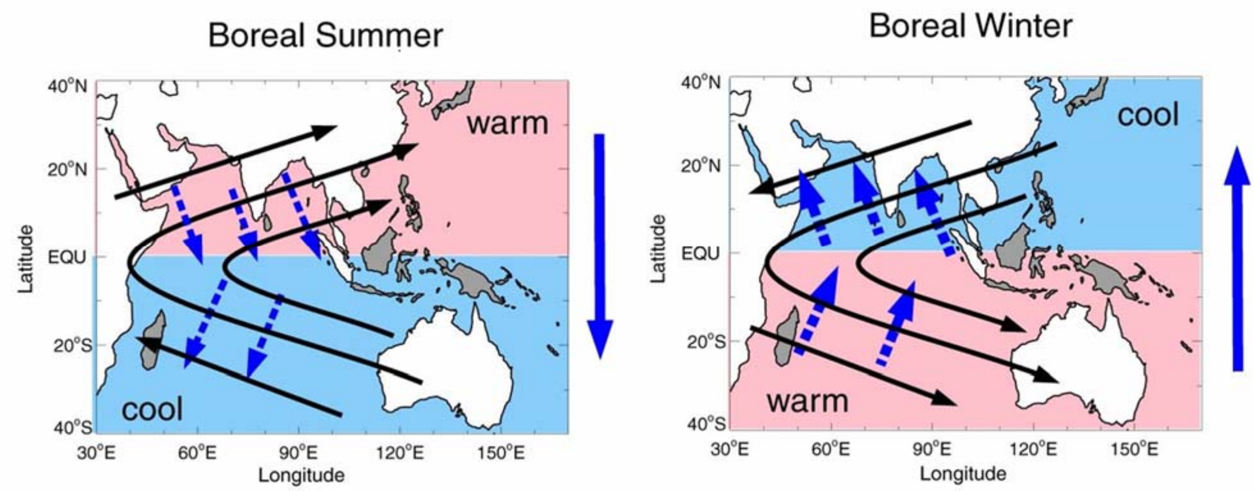

Fig. 4.18 Annually reversing Indian Ocean-monsoon system. The summer-winter hemispheric temperature difference enforces monsoon (curved black arrows), which induces the Ekman transports (blue dashed arrows). The net ocean heat transport (blue solid arrows to the right of the panels) relaxes the summer-winter difference. (Webster et al., 2002).

over the maritime continent is not so uniquely dominant as in the extratropics, and these are why the climatological description could not be done until 1980s in spite of about 2,000 rain gauge stations constructed until the end of 19th century. Many high (often active) volcanoes and deep jangles have been covered by neither old rain gauge nor recent radar networks, which are also related to the modifications of intraseasonal variations over the maritime continent. Due to asymmetrically gigantic and small continents, Eurasia and Australia, the northward invasions of the ITCZ and boreal summer monsoon are deeper (at least zonal mean) than the southward one with boreal winter monsoon, but the latter (the cold surge) may cause torrential rainfalls along the western coast of the South China Sea (Vietnam and Malay) and in the western maritime continent, in particular when synoptic-scale cyclonic disturbances are formed near Kalimantan and southern Philippines (*e.g.*, Cheang, 1977; Murakami and Matsumoto, 1994; Tangang and Juneng, 2004; Wu et al., 2007, 2011; Yokoi and Matsumoto, 2008; Hattori et al., 2011; Chen et al., 2013, 2015; Matsumoto et al., 2017) by amplifying local diurnal cycles (as will be mentioned in Section 6.1), together with interannual variations (see Section 6.3). Such superimposition of multiple scales makes complex features of seasonal march over this region.

The atmosphere and ocean are interacting with each other through the monsoon. On one hand, because the (primary 'geographical' component of) monsoon circulation is driven by the continent-ocean temperature gradient, it is quite sensitive to variations of the sea surface temperature which are known to appear actually and dominantly associated with interannual variations (Section 5.3). On the other hand, because a sufficiently strong and almost unidirectional wind may drive the surface ocean through the Ekman friction, the sea surface temperature field may be affected by the monsoon. Therefore the monsoon and the surface ocean are interacting, and the summer-winter temperature difference is suppressed through this interaction (Fig. 4.18) (see e.g., Webster et al., 1998, 2002).

Recent very rapid industrial development over the monsoon Asia may cause extension of air pollutant (gases and aerosols) over broad regions by monsoons, and also interactions between monsoon and aerosols (e.g., Lau et al., 2006; Reid et al., 2013). For example, some aerosols such as black carbon may induce heating of the atmosphere by absorption of insolation, which is opposite to the parasol effect of the other aerosols. They are emitted massively in

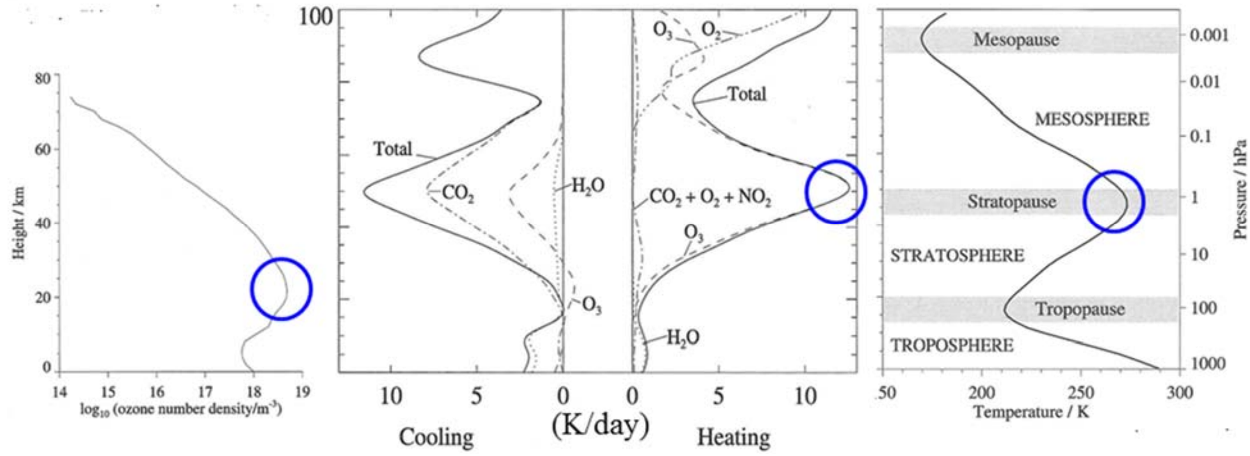

Fig. 4.19 Ozone number density, radiative cooling/heating with minor constituents and definition of atmospheric vertical regions by the standard temperature profile (from left to right). Copied from Andrews (2000), based on the CIRA 1986 standard atmosphere (Rees et al., 1990).

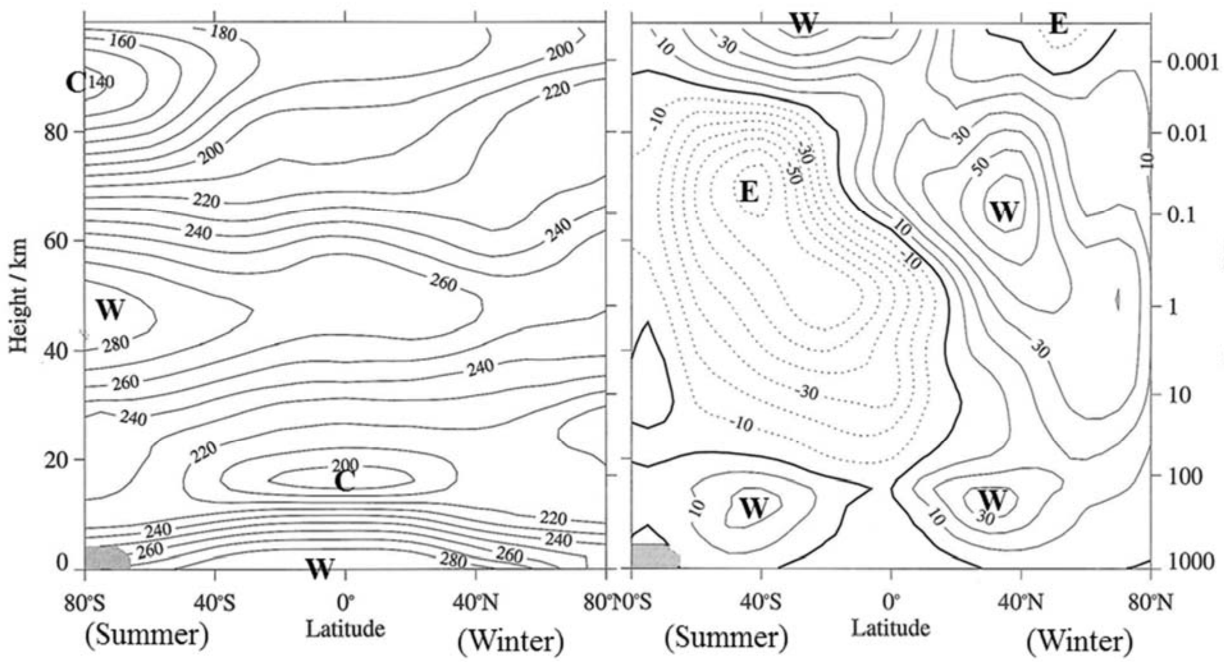

Fig. 4.20 The meridional distributions of zonal-mean temperature (left) and zonal wind (right) of the CIRA 1986 standard atmosphere for January (Rees et al., 1990).

the Indian subcontinent, and transported northward and upward by the summer monsoon circulation to the middle troposphere over the Tibetan Plateau. Their heating intensifies the monsoon, which makes a positive feedback to the increase of aerosols.

4.5. Brewer-Dobson circulation

In the 'middle atmosphere' or the stratosphere and mesosphere (cf. Section 3.2), photochemical processes of minor constituents such as ozone are essentially important (Fig. 4.19). The amount of ozone is too much more than for absorbing the solar ultraviolet radiation, and the resulting vertically temperature maximum or the stratopause is separated clearly upward from the ozone maximum altitude. The production of ozone is associated with the ultraviolet

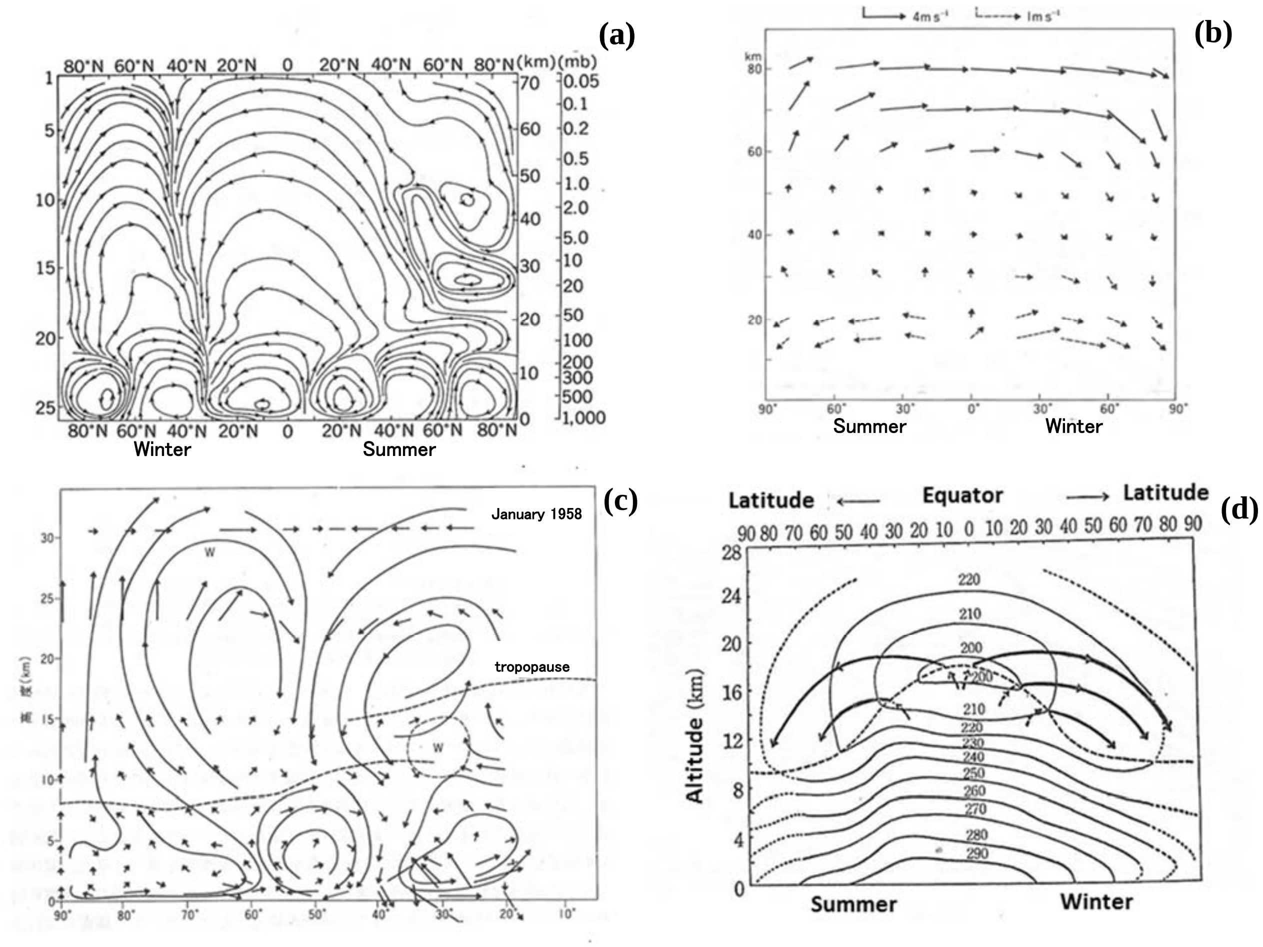

Fig. 4.21 Meridional circulations in usual Eulerian zonal-mean (left two) and those corresponding to transformed Eulerian mean (right two) for the whole lower-middle atmosphere (upper two) and the troposphere-lower stratosphere (lower two): (a) a numerical model for by Cunnold et al. (1975); (b) qualitative estimation by Prof. Matsuno from radiative imbalance (Murgatroyd and Singleton, 1961); (c) Northern hemispheric winter analysis by Miyakoda (1963) obtained through Prof. Matsuno; and speculation based on water vapor distribution by Brewer (1949).

component dependent on the total insolation, and this is why the highest stratopause temperature appears at the summer pole (Fig. 4.20) with the strongest insolation (Fig. 4.5). However, the equatorial region with insolation intensity next to the summer pole is not so much ozone and not so warm, and the winter pole with no insolation has ozone and stratopause, which suggests that dynamical processes transporting ozone and heat from summer hemisphere to winter hemisphere are also important. For the bottom of the stratosphere or the tropopause is the highest in altitude and the coldest in temperature (Figs. 4.2 and 4.20), which is determined by the radiative-convective equilibrium. The mean zonal wind above the upper limit of usual radiosonde and wind profiler observations is usually derived from the satellite-observed temperature field, based on the thermal wind equilibrium (Section 4.1). Therefore easterly and westerly are distributed in the summer and winter hemispheres, respectively[34], although the equatorial region between the both hemispheres has downward propagating variations of quasi-biennial and semiannual periods in the lower-middle stratosphere and around the stratopause/mesopause, respectively (Section 5.4).

[34]Without mechanical forcing (friction and/or wave stress to be mentioned later), there may be no meridional circulation (thus no troposphere-stratosphere tropics-extratropics exchanges) and a zonal-mean zonal flow satisfying completely the thermal wind equilibrium with the meridional temperature gradient induced by the radiative heating as mentioned in Section 4.1.

Brewer (1949) and Dobson (1956) analyzed minor but well conserved constituent distributions, and speculated a circulation ascending from the equatorial tropopause, flowing both poleward in the lower stratosphere and descending through the both polar tropopauses (Fig. 4.21(d)), which is like upward-shifted Hadley's original circulation. For example, the extratropical stratosphere is extremely dry, because the whole air passes the coolest (often −80ºC or lower) equatorial tropopause and almost all the water vapor is exhausted as ice particles falling as rain on the ground[35]. Many studies during 1970s−80s revealed that the intrusion of water vapor into the stratosphere is concentrated in the most active convection region around the Indonesian maritime continent[36], and that the turn-over time to replace the stratospheric air is about 2 years. Contribution of this Brewer-Dobson circulation to the ozone and related manor constituents which are essentially important in the stratospheric structure and dynamics was also revealed. Through this circulation the tropical troposphere is directly connected to the extratropical lower stratosphere, and these two regions are regarded as one "middle world" (Holton et al., 1995).

Radiation studies suggested an imbalance of purely radiative energy budget in the middle atmosphere (Fig. 4.21(b)), which requested a meridional circulation above around the stratopause to transport heat from the overheated summer hemisphere to the overcooled winter hemisphere, and another one in the lower stratosphere to cool and heat the equatorial and polar tropopauses, respectively, than those expected in case of no motions. The former is similar to the globally one-cell 'astronomical' monsoon considered in Section 4.4, and the latter is just like the hemispherically one-cell Brewer-Dobson circulation speculated from the mass transport. Anyway those middle-atmospheric circulations appear clearly only in each uppermost flow, and the other parts cannot be seen actually because of weaker velocity to compensate the larger atmospheric density with mass conservation.

However, actual (Eulerian) zonal mean meridional circulation ($\overline{v}$, $\overline{w}$) in the lower stratosphere has two cells in each hemisphere: a thermally direct cell in the lower latitudes and an indirect cell in the higher latitudes, which are like upward extensions of Hadley and Ferrel circulations, respectively (Fig. 4.21(a), (c)), and are not identical to the hemispherically one-cell Brewer-Dobson circulation. As mentioned in Section 4.2 (p. 39), this is because the forcings $\overline{G}$ and $\overline{Q}$ involve quadratic (nonlinear) terms due to non-axi-symmetric disturbances. In the extratropical troposphere such disturbances are unsteady (due to a baroclinic instability), and the Ferrel circulation appears always, although its contribution on mass transport is diffusive rather than advective (see, e.g., Kida, 1983a,b). In the high-latitude stratosphere, such disturbances are almost steady (associated with Rossby waves (Section 5.1) forced in the troposphere by continent-ocean distributions), and do not contribute to the mass transport.

Andrews and McIntyre (1976) introduced the *transformed Eulerian mean* (TEM) formulation providing the transport processes in the meridional plane more directly. Incorporating the eddy meridional heat flux in the heating term $\overline{Q}$ to satisfy the continuity equation (4.5):

$$\overline{v}^* \equiv \overline{v} - \frac{1}{\rho_0}\frac{\partial\left(\rho_0\overline{T'v'}/N^2\right)/\partial z}{H/R} \equiv -\frac{1}{\rho_0}\frac{\partial\overline{\psi}^*}{\partial z}, \quad \overline{w}^* \equiv \overline{w} + \frac{1}{\rho_0}\frac{\partial\left(\rho_0\overline{T'v'}/N^2\right)/\partial y}{H/R} \equiv \frac{1}{\rho_0}\frac{\partial\overline{\psi}^*}{\partial y}, \tag{4.24}$$

we obtain a *transformed Eulerian mean* (TEM) meridional circulation concerning only one dependent variable $\overline{\psi}^*$:

$$\frac{\partial^2\overline{\psi}^*}{\partial y^2} + \frac{f^2}{N^2}\rho_0\frac{\partial}{\partial z}\left(\frac{1}{\rho_0}\frac{\partial\overline{\psi}^*}{\partial z}\right) = \frac{\rho_0}{N^2}\left[\frac{\partial}{\partial y}\left(\frac{R}{H}\frac{\overline{J}}{C_p}\right) + f\frac{\partial\overline{G}^*}{\partial z}\right], \tag{4.25}$$

[35]This is the so-called the 'cold trap' mechanism playing the most essential role to keep the water on Earth.
[36]Newell and Gould-Stewart (1981) called this "stratospheric fountain".

where

$$\overline{G}^* \equiv \overline{F_x} + \frac{1}{\rho_0}\left(\frac{\partial \overline{E}_y}{\partial y} + \frac{\partial \overline{E}_z}{\partial z}\right), \quad \overline{E}_y \equiv -\rho_0 \overline{u'v'}, \quad \overline{E}_z \equiv -\rho_0 \left(\overline{u'w'} + \frac{fR}{HN^2}\overline{T'v'}\right) \tag{4.26}$$

and $(\overline{E}_y,\ \overline{E}_z)$ is called the *Eliassen-Palm flux*, after a pioneering study on wave-mean flow interaction by Eliassen and Palm (1961). (4.25) implies that the mass transport expressed by a TEM meridional circulation $\overline{\psi}^*$ is driven by the mechanical forcing given by the Eliassen-Palm flux divergence.

Some features of the Brewer-Dobson circulation derived from (4.25) are mathematically similar to those of the Hadley circulation (or its original one-cell model) from (4.23) or its simplified version (4.20). Diabatic heating/cooling excesses $\overline{J}$ near the equator/poles induce TEM upward/downward flows $\overline{w}^*$. The eddy (wave-induced) heat flux involved in $\overline{Q}$ making usual Eulerian zonal mean vertical flow $\overline{w}$ does not produce any TEM vertical flow $\overline{w}^*$, but may produce TEM meridional flow $\overline{v}^*$ through the Eliassen-Palm flux divergence in $\overline{G}^*$. Therefore the Brewer-Dobson circulation is also a circulation forced by the extratropical wave effect.

Together with the diagnostic equation (4.25), we may use a time evolution equation similar to the Ertel potential vorticity equation (4.15) in the usual zonal mean system: in a good approximation,

$$\frac{\partial \overline{P_g}}{\partial t} = -\frac{\partial \overline{P_g{}'v'}}{\partial y} + \frac{Rf_0}{HN^2\rho_0}\frac{\partial}{\partial z}\rho_0 e^{-(R/C_pH)z}\frac{\overline{J}}{C_p}, \tag{4.27}$$

$$\overline{P_g} \equiv f_0 + \beta y - \frac{\partial \overline{u}}{\partial y} + \frac{Rf_0}{HN^2\rho_0}\frac{\partial \rho_0 \overline{T}}{\partial z}, \quad \overline{P_g'v'} \equiv \frac{1}{\rho_0}\left(\frac{\partial \overline{E}_y}{\partial y} + \frac{\partial \overline{E}_z}{\partial z}\right), \tag{4.28}$$

where P_g is called geostrophic potential vorticity, and $f_0 = f(y = 0)$ is a reference value of the Coriolis parameter in the β-plane approximation. For the equatorial β-plane approximation (4.7), $f_0 = 0$ and $\overline{P_g} \equiv \beta y - \partial\overline{u}/\partial y$. (4.27) is a governing equation for the wave-mean flow interaction (Section 5.4), and essentially the same as used in the numerical prediction (cf. Chapter 10 of Holton (1992) and Chapter 3 of Andrews et al. (1987)). .

Physical meanings and concrete expressions of the Eliassen-Palm flux $(\overline{E}_y,\ \overline{E}_z)$ will be described in Section 5.4, but here for understanding the meridional circulations it should be noted that $(\overline{E}_y,\ \overline{E}_z)$ is mainly due to transient large-scale (amplifying Rossby or decaying tropospheric baroclinic) waves and mesoscale (gravity) waves. For the latter, Tanaka and Yamanaka (1985) showed that almost stationary gravity waves generated by the surface topography should be breaking and making $\overline{G}^* < 0$ in the lower stratosphere, which contributes to maintenance of the Brewer-Dobson circulation and the weak wind layer there. Similar scheme is used as the gravity wave drag in almost all the (both global and regional) numerical models including the tropics (e.g., Palmer et al., 1986; Iwasaki et al., 1989a, b). Because stationary waves are “absorbed” below the middle stratosphere, survived eastward/westward propagating waves propagate into the mesosphere and above, which induce weak wind layer and summer-to-winter meridional circulation near the mesopause and inversed zonal wind in the lower thermosphere (Matsuno, 1982; Lindzen,1981; Holton, 1982).

Exercise 4

(1) Derive the β-plane approximation (4.7) from the definition of Coriolis parameter: $f = 2\Omega \sin\varphi$ shown in Chapter 2.

(2) The Earth's rotation is with the angular velocity $\Omega = 2\pi/86164$s, or with a period of 86164 s. Why this 86164 s is shorter than 1 day (= 24 h = 24x60x60 s = 86,400 s) ?

(3) Estimate the eastward speed of the equatorial ground with the Earth's rotation. How about in the mid-latitude (e.g. 45º)? How different the Coriolis force in the northern and southern hemispheres? How about at the equator?

(4) Do you think the motorcycle rider and the bathtub vortex must feel the Coriolis force of the earth's rotation? How about the Coriolis for the solar system, or of galaxy?

Answers:

(1) From the definition, $f = 2\Omega \sin\varphi$, and $y = a\varphi$. Then

$$\beta = df/dy = (1/a)\, df/dy = (2\Omega/a) \cos\varphi$$

At the equator ($\varphi = 0$), we have $\beta = 2\Omega/a$.

(2) 1 day is defined with the sun observed at the Earth. Because the Earth is rotating around the sun one time during 365 times of self-rotation, that is, in total 365 + 1 = 366 times per year. So the rotation period becomes 86400 s × 365/366 ≈ 86161 s.

(3) The circumference of latitude φ is given by $2\pi\, a \cos\varphi$. This circle is rotating eastward by the Earth's rotation with an angular velocity Ω (unit: radian/s), or the period of $2\pi/\Omega$ (unit: s). Thus the speed of ground is

$$2\pi\, a \cos\varphi \;/\; (2\pi/\Omega) = a\, \Omega \cos\varphi.$$

Using $a \approx 6.4 \cdot 10^3$ km $= 6.4 \cdot 10^6$ m and $\Omega = 2\pi/86164\text{s} \approx 7.3 \cdot 10^{-5}\ \text{s}^{-1}$, we have

$a\,\Omega \approx 4.7 \cdot 10^2$ m/s at the equator, and

$a\,\Omega \times 1/\sqrt{2} \approx 3.3 \cdot 10^2$ m/s at $\varphi = 45°$.,

which are sufficiently faster than usual wind speed (relative to the Earth).